

## CORONAVIRUS

# Serial interval of SARS-CoV-2 was shortened over time by nonpharmaceutical interventions

Sheikh Taslim Ali<sup>1\*</sup>, Lin Wang<sup>2,3\*</sup>, Eric H. Y. Lau<sup>1\*</sup>, Xiao-Ke Xu<sup>4</sup>, Zhanwei Du<sup>5</sup>, Ye Wu<sup>6,7</sup>, Gabriel M. Leung<sup>1</sup>, Benjamin J. Cowling<sup>1†</sup>

Studies of novel coronavirus disease 2019 (COVID-19), which is caused by severe acute respiratory syndrome coronavirus 2 (SARS-CoV-2), have reported varying estimates of epidemiological parameters, including serial interval distributions—i.e., the time between illness onset in successive cases in a transmission chain—and reproduction numbers. By compiling a line-list database of transmission pairs in mainland China, we show that mean serial intervals of COVID-19 shortened substantially from 7.8 to 2.6 days within a month (9 January to 13 February 2020). This change was driven by enhanced nonpharmaceutical interventions, particularly case isolation. We also show that using real-time estimation of serial intervals allowing for variation over time provides more accurate estimates of reproduction numbers than using conventionally fixed serial interval distributions. These findings could improve our ability to assess transmission dynamics, forecast future incidence, and estimate the impact of control measures.

In December 2019, a novel coronavirus disease [coronavirus disease 2019 (COVID-19)], caused by severe acute respiratory syndrome coronavirus 2 (SARS-CoV-2), was first reported in Wuhan, China. It has since spread to more than 212 countries, causing more than 10 million confirmed cases and 500,000 deaths worldwide as of 30 June 2020 (1). Recent studies have suggested that several demographic and social factors can influence the transmission of COVID-19, including age- and gender-related differences in infection risk (2–4), reduced risk of infection as a result of intensive nonpharmaceutical interventions (NPIs) (e.g., isolation and social distancing) (5–7), and abrupt changes in social mixing patterns because of lockdowns and confinement (8–10). Serial interval, defined as the duration between the symptom-onset time of the infector and that of the infectee, is an essential metric for estimating many other key epidemiological parameters (e.g., reproduction number, generation time, and attack rate), which are used in turn to predict disease trends and health care demands (11). In early studies, before the availability of specific data on COVID-19, the serial interval distribution of COVID-19 was assumed to be similar to those of severe acute respiratory syndrome (SARS) or Middle East respiratory syndrome (MERS), with a mean >8 days (12, 13). Once specific data became available on COVID-19 transmission pairs, several studies examined the serial interval distribution of COVID-19 in different locations, with estimates of the mean

serial interval varying from 3.1 to 7.5 days (6, 14–21). All of these studies have assumed that the timing of transmission events can be described by a single, stable distribution of serial intervals at different stages of an epidemic.

In fact, the serial interval depends on the incubation period, the profile of infectiousness after infection, and the variation in contact structure of the population (as explained in fig. S1) (22). The incubation period describes the biological process of disease progression and tends to follow a more similar distribution from one location to another, with minor variations resulting from social or cultural differences in how symptoms are perceived or reported. However, the profile of infectiousness over time can vary because of human behavior. Changes in contact patterns and the use of public health measures can reshape the timing of infection events by limiting successful contacts overall (e.g., social distancing) or after illness onset (e.g., case isolation). Interventions such as the isolation of confirmed and suspected cases, suspension of intra- and intercity travel, and different forms of social distancing were widely implemented in different Chinese cities. This provides an opportunity to study the temporal changes in the serial interval distribution and its association with NPIs. Here, we show that variation in the serial interval can occur and has important implications for the assessment of transmission dynamics and the impact of control measures.

We compiled a database of 1407 COVID-19 transmission pairs, in which symptom-onset dates and social relationships were available for both the infector and infectee of 677 transmission pairs [see table S1 for entire database (23) and supplementary materials for details]. Household and nonhousehold transmissions were identified on the basis of the information on social relationships (e.g., familial members of the same household, non-household relatives, colleagues, classmates, friends, and other face-to-face contacts). The data were reconstructed from the publicly available reports of 9120 confirmed COVID-19 cases reported by 27 provincial and 264 urban health commissions in China outside Hubei province. Data from Hubei province were excluded because there was less reliable information on chains of transmission during the widespread community circulation of COVID-19; outside Hubei province, it was more straightforward to link connected cases and derive serial intervals. We focused on 677 transmission pairs with infectors having developed symptoms from 9 January through 13 February 2020. This 36-day period spans a series of key interventions related to the evolving epidemiology and transmission dynamics of COVID-19 in mainland China (24–26).

We first calculated the number of transmission pairs in our database by the onset dates of infectors (fig. S3). Because many infectors (339) developed symptoms during 23 to 29 January 2020, we defined this 1-week period as the peak week, the previous 14-day period (9 to 22 January 2020) as the prepeak period, and the following 15-day period (30 January to 13 February 2020) as the postpeak period. We computed the serial interval as the number of days between the symptom-onset date of the infector and that of the infectee for each transmission pair. Empirical serial interval distributions for transmission pairs, counting from symptom onsets of the infectors during each period, indicate that the serial intervals shortened over time (Fig. 1A).

We estimated the serial interval distribution during each nonoverlapping period by fitting a normal distribution to the corresponding serial intervals data (supplementary materials). Analysis of all 677 transmission pairs revealed that the serial interval distribution had a mean of 5.1 [95% credibility interval (CrI): 4.7, 5.5] days and a standard deviation (SD) of 5.3 (95% CrI: 5.0, 5.6) days (table S2) overall, which is consistent with other recent

<sup>1</sup>WHO Collaborating Centre for Infectious Disease Epidemiology and Control, School of Public Health, Li Ka Shing Faculty of Medicine, The University of Hong Kong, Hong Kong Special Administrative Region, China. <sup>2</sup>Department of Genetics, University of Cambridge, Cambridge CB2 3EH, UK. <sup>3</sup>Mathematical Modelling of Infectious Diseases Unit, Institut Pasteur, UMR2000, CNRS, Paris 75015, France. <sup>4</sup>College of Information and Communication Engineering, Dalian Minzu University, Dalian 116600, China. <sup>5</sup>Department of Integrative Biology, University of Texas at Austin, Austin, TX 78705, USA. <sup>6</sup>School of Journalism and Communication, Beijing Normal University, Beijing 100875, China. <sup>7</sup>Computational Communication Research Center, Beijing Normal University, Zhuhai 519087, China.

\*These authors contributed equally to this work.

†Corresponding author. Email: bcowling@hku.hk

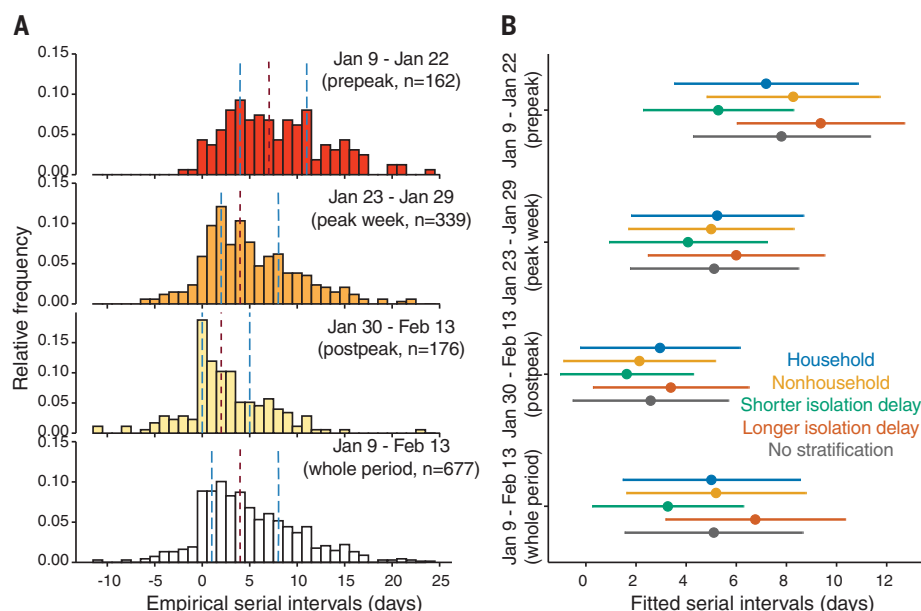


**Fig. 1. Serial intervals of SARS-CoV-2 substantially shortened over time in mainland China.** (A) Empirical serial interval distributions. From top to bottom, transmission pairs were analyzed by selecting infectors who developed symptoms during 9 to 22 January 2020 (prepeak); 23 to 29 January 2020 (peak week); 30 January to 13 February 2020 (postpeak); and 9 January to 13 February 2020 (whole period), respectively. In each panel, vertical dashed lines in red and blue colors indicate the median and interquartile range (IQR), respectively. (B) Estimated serial interval distributions by fitting a normal distribution using MCMC. From top to bottom, each group of bars corresponds to the transmission pairs with infectors who developed symptoms during the prepeak (162 pairs), peak week (339 pairs), postpeak (176 pairs), and whole 36-day period (677 pairs), respectively. Colored dots and bars correspond to the transmission pairs within households (blue), outside households (yellow), with isolation delays shorter than the median isolation delay of each period (green), and with isolation delays longer than the median isolation delay of each period (orange), respectively. Dark gray bars correspond to transmission pairs with no stratification. Dots and bars indicate the estimated median and IQR, respectively.

studies (16, 21, 27). However, fitting to data of nonoverlapping periods of time revealed considerable variation in serial interval distributions (Fig. 1B). Before the peak, the mean and SD of serial intervals were estimated to be 7.8 (7.0, 8.6) days and 5.2 (4.7, 5.9) days, respectively. During the peak, the mean and SD reduced to 5.1 (4.6, 5.7) days and 5.0 (4.6, 5.4) days, respectively. After the peak, these estimates further shortened to 2.6 (1.9, 3.2) days and 4.6 (4.2, 5.1) days, respectively (table S2).

Next, we examined the real-time change in serial intervals by using a series of running time windows with fixed lengths of 10, 14, or 18 days (fig. S10). In contrast to the use of a constant distribution of serial intervals, our analysis suggests that serial intervals were gradually shortened over the study period (Fig. 2A), which is robust to alternative specifications of time windows (fig. S10). By fitting the transmission pairs data for each running time window by Markov chain Monte Carlo (MCMC) (Fig. 2A and table S3), we estimated that during the first 14-day period (9 to 22 January 2020), the serial intervals were longer on average [mean: 7.8 (95% CrI: 7.0, 8.6) days; SD: 5.2 (95% CrI: 4.7, 5.9) days];

whereas during the last 14 days (30 January to 13 February 2020), the serial intervals were much shorter on average [mean: 2.2 (1.5, 2.9) days; SD: 4.6 (4.1, 5.1) days]. Notably, the mean serial intervals were shortened by more than a factor of 3 over the 36-day period.

The transmission pair data also contain information for age, sex, household, and isolation delay (i.e., time duration from symptom onset to isolation) for most infectors. This allows for a granular stratification. Using either nonoverlapping or running time windows for data stratified by each of these factors, we find the same pattern of shorter serial intervals over time (Figs. 1B and 2A and tables S2 and S3). Therefore, we termed this changing serial interval the effective serial interval, which accounts for temporal changes caused by its potential driving factors. Notably, the length of effective serial intervals is positively associated with the length of isolation delay (Fig. 2A; figs. S5, S6, and S9; and tables S3 and S4), which accounts for the decreasing isolation delay over time (fig. S2). Therefore, early isolation (shorter than the median isolation delay) translates into shorter serial intervals [mean: 3.3 (2.7, 3.8) days; SD: 4.5 (4.1, 4.9) days], and de-

layed isolation (longer than the median isolation delay) is associated with longer serial intervals [mean: 6.8 (6.2, 7.3) days; SD: 5.3 (4.9, 5.7) days] (table S2). Stratification by age, gender, or household shows no clear differences in serial interval estimates. Our findings are robust to using alternative distributions (e.g., Gumbel distribution) for model fitting (fig. S11) and the infector-based approach (fig. S14).

Our probabilistic, individual-based simulated and regression models confirm that serial intervals are positively associated with isolation delay (section 5, supplementary materials). We found that the serial intervals become shorter on the basis of how much faster the infectors are isolated, regardless of when an infector starts to be infectious before symptom onset (fig. S5). In an individual-based simulation model with a mean generation time of 7.8 days, the simulated mean serial intervals are reduced from ~8.0 to ~1.2 days when the isolation delay is reduced from 10 to 0 days. We found through regression models that up to 51.5% of the variability in daily empirical serial interval can be explained by isolation delay and further improved by other NPI factors, which explain an additional 15.6 to 16.7% of the variability (table S5).

In practice, the time-varying serial interval may affect the estimation of epidemic parameters, including the transmissibility. The real-time transmissibility of an infectious disease is often characterized by the instantaneous reproduction number ( $R_t$ ), which is defined as the expected number of secondary infections caused by an infector on day  $t$ . The pathogen spreads when  $R_t > 1$  and is under control when  $R_t < 1$ . To examine the effect of serial intervals on  $R_t$ , we first obtained the daily number of cases on the basis of the onset dates of infectors and infectees among the 1407 transmission pairs (Fig. 2, B to D). By applying the statistical method developed by Cori *et al.* (28), we estimated  $R_t$  for each day between 20 January and 13 February 2020. We noticed substantial differences in estimates of  $R_t$  between using a single stable serial interval distribution and time-varying effective serial interval distributions. The magnitude of this difference is more prominent during the prepeak and postpeak periods than it is during the peak week when  $R_t \approx 1$  (Fig. 2, B to D).

We observed that the serial interval for COVID-19 in mainland China was shortened by more than a factor of 3 in the 36 days between 9 January and 13 February 2020. This reduction was driven by intensive NPIs, particularly the reduction of the isolation delay period. Isolation of an infector 1 day earlier is expected to reduce the mean serial interval by 0.7 days. Thus, the serial interval was shortened by >3 days if infectors were rapidly isolated (Figs. 1B and 2A and tables S2 and S3). This is consistent with advocating isolation of cases

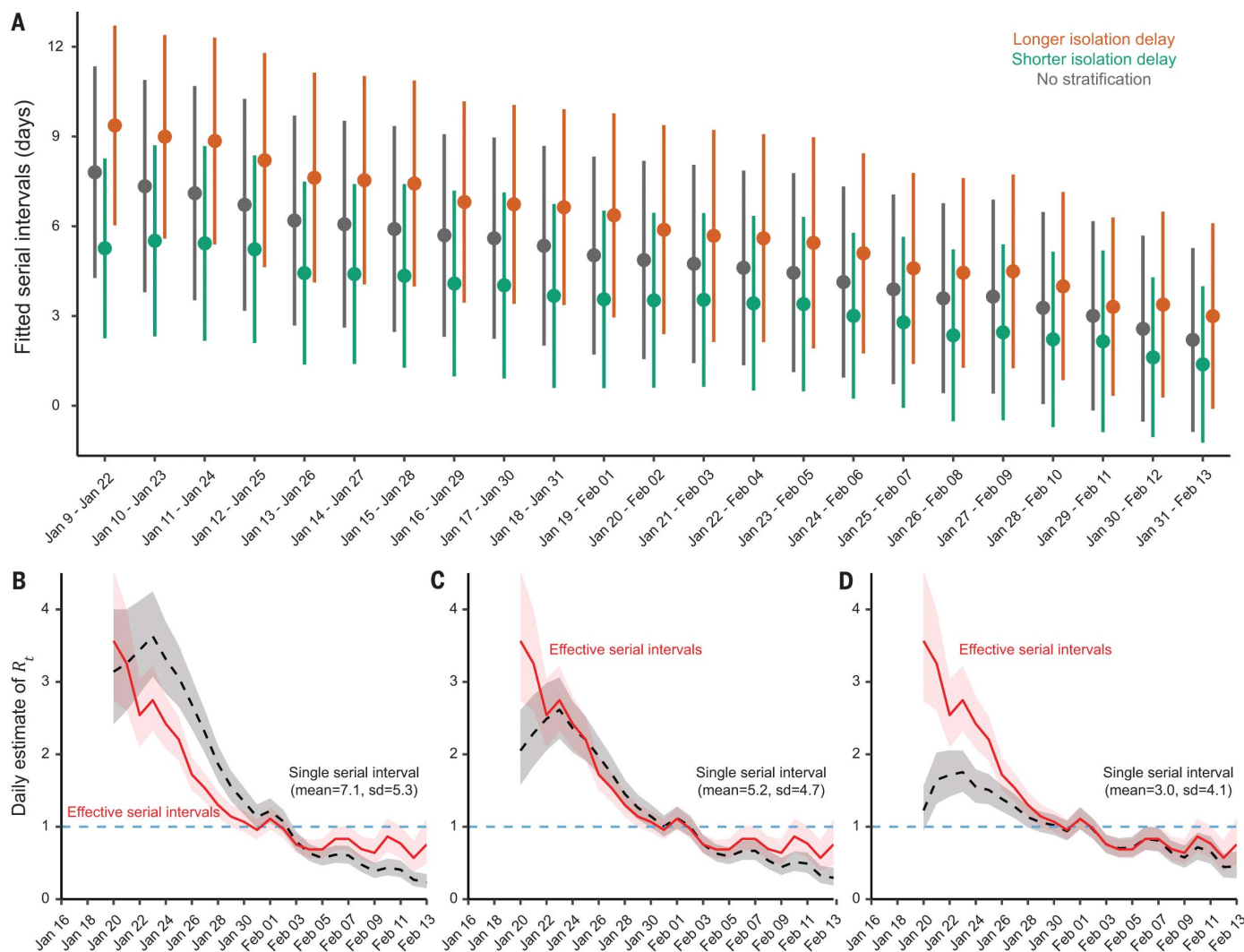


**Fig. 2. Real-time effective serial intervals and instantaneous reproduction number  $R_t$ .** (A) Estimated serial interval distribution for each 14-day running time window. Dark gray color indicates fitting data with no stratification, whereas green and orange indicate fitting data with isolation delay shorter and longer, respectively, than the median isolation delay of each running time window. Dots and bars indicate the estimated median and IQR, respectively. (B to D) Daily estimates of  $R_t$  by using real-time effective serial interval distributions [as in (A)]

versus using a single fixed serial interval distribution. Red curves and light pink shaded regions indicate the median and 95% CrI, respectively, of daily  $R_t$  estimated using real-time effective serial interval distributions. Black dashed curves and light gray shaded regions indicate the median and 95% CrI, respectively, of daily  $R_t$  estimated using a single serial interval distribution fixed, with a mean of 7.1 and SD of 5.3 days in (B), a mean of 5.2 and SD of 4.7 days in (C), and a mean of 3.0 and SD of 4.1 days in (D).

and quarantining contacts within 1 day from symptom onset, which has been estimated to reduce COVID-19 transmission by 60% (8). We have not identified any substantial effects of gender or age of infectors on serial interval, but the NPIs were found to be significant for the transmission in communities rather than in households (table S5). Other studies (15, 20) have estimated that the infectiousness of COVID-19 is greater at symptom onset. Although a short serial interval indicates that a substantial proportion of transmission events have occurred by the time symptoms are apparent (14), because of prolonged viral shedding (14, 29, 30) case isolation is still likely to reduce further transmission. Changes in the

serial interval can therefore indicate effective implementation of specific transmission-reduction measures.

There are some limitations to our work. First, it is possible that there was recall bias on the onset of first symptoms in the line-list data; however, given the centralized pandemic response in mainland China, we expected that recall bias would not affect our main conclusions (figs. S12 and S13). Second, other factors may have influenced the reduction of effective serial intervals, as we can only explain up to 72% of the variance in observed serial intervals. Finally, our current transmission pair data do not contain variables about the potential exposure window of each case, which do

not allow further inferences on the transmission potential.

Our results indicate that caution is needed when attempting to generalize estimates of the serial interval distribution to other places or to other periods of time in the same place, for example when estimating instantaneous reproductive numbers (Fig. 2, B to D). The real-time metric of effective serial intervals indicates that transmission models also need to account for the temporal variation in serial intervals as an epidemic proceeds. Effective serial intervals may provide better measurements of instantaneous transmissibility ( $R_t$ )—because they include the effects of possible drivers of transmission—and could be helpful

to policy-makers because they offer real-time information on the impact of public health measures.

## REFERENCES AND NOTES

- World Health Organization (WHO). "Coronavirus disease 2019 (COVID-19): Situation report – 162" (WHO, 2020); [www.who.int/docs/default-source/coronaviruse/situation-reports/20200629-covid-19-sitrep-161.pdf?sfvrsn=74fde64e\\_2](http://www.who.int/docs/default-source/coronaviruse/situation-reports/20200629-covid-19-sitrep-161.pdf?sfvrsn=74fde64e_2).
- M. U. G. Kraemer *et al.*, *Science* **368**, 493–497 (2020).
- C. Wenham, J. Smith, R. Morgan, Gender and COVID-19 Working Group, *Lancet* **395**, 846–848 (2020).
- J. M. Jin *et al.*, *Front. Public Health* **8**, 152 (2020).
- J. Hellewell *et al.*, *Lancet Glob. Health* **8**, e488–e496 (2020).
- L. Ferretti *et al.*, *Science* **368**, eabb6936 (2020).
- R. Armitage, L. B. Nellums, *Lancet Public Health* **5**, e256 (2020).
- R. M. Anderson, H. Heesterbeek, D. Klinkenberg, T. D. Hollingsworth, *Lancet* **395**, 931–934 (2020).
- J. R. Koo *et al.*, *Lancet Infect. Dis.* **20**, 678–688 (2020).
- K. Prem *et al.*, *Lancet Public Health* **5**, e261–e270 (2020).
- M. A. Vink, M. C. Bootsma, J. Wallinga, *Am. J. Epidemiol.* **180**, 865–875 (2014).
- J. T. Wu, K. Leung, G. M. Leung, *Lancet* **395**, 689–697 (2020).
- M. Chinazzi *et al.*, *Science* **368**, 395–400 (2020).
- H. Nishiura, N. M. Linton, A. R. Akhmetzhanov, *Int. J. Infect. Dis.* **93**, 284–286 (2020).
- H. Y. Cheng *et al.*, *JAMA Intern. Med.* 10.1001/jamainternmed.2020.2020 (2020).
- Z. Du *et al.*, *Emerg. Infect. Dis.* **26**, 1341–1343 (2020).
- Q. Li *et al.*, *N. Engl. J. Med.* **382**, 1199–1207 (2020).
- J. M. Griffin *et al.*, *medRxiv* 2020.05.08.20095075 [Preprint]. 11 May 2020. <https://doi.org/10.1101/2020.05.08.20095075>.
- S. Ma *et al.*, *medRxiv* 2020.03.21.20040329 [Preprint]. 24 March 2020. <https://doi.org/10.1101/2020.03.21.20040329>.
- X. He *et al.*, *Nat. Med.* **26**, 672–675 (2020).
- Q. Bi *et al.*, *Lancet Infect. Dis.* **20**, 911–919 (2020).
- J. Zhang *et al.*, *Science* **368**, 1481–1486 (2020).
- Lin, PDGLin/COVID19\_EffSerialInterval\_NPI: Serial interval of SARS-CoV-2 was shortened over time by non-pharmaceutical interventions, version v1.0, Zenodo (2020); <https://doi.org/10.5281/zenodo.3940300>.
- H. Tian *et al.*, *Science* **368**, 638–642 (2020).
- K. Leung, J. T. Wu, D. Liu, G. M. Leung, *Lancet* **395**, 1382–1393 (2020).
- A. Pan *et al.*, *JAMA* **323**, 1915–1923 (2020).
- J. Zhang *et al.*, *Lancet Infect. Dis.* **20**, 793–802 (2020).
- A. Cori, N. M. Ferguson, C. Fraser, S. Cauchemez, *Am. J. Epidemiol.* **178**, 1505–1512 (2013).
- L. Zou *et al.*, *N. Engl. J. Med.* **382**, 1177–1179 (2020).
- Y. Pan, D. Zhang, P. Yang, L. L. M. Poon, Q. Wang, *Lancet Infect. Dis.* **20**, 411–412 (2020).

## ACKNOWLEDGMENTS

We thank all the health workers and volunteers who collected data throughout the COVID-19 outbreak. We thank H. Salje, S. Cauchemez, L. A. Meyers, J. Paireau, Q. Bi, B. Yang, X. Liu, and L. Hu for discussions. **Funding:** We acknowledge financial support from the Health and Medical Research Fund, Food and Health Bureau, Government of the Hong Kong Special Administrative Region, China (grant no. COVID190118); the Investissement d'Avenir program, the Laboratoire d'Excellence Integrative Biology of Emerging Infectious Diseases program (grant no. ANR-10-LABX-62-IBED); the European Research Council (grant no. 804744); the European Union's Horizon 2020 research and innovation program under grant agreement no. 101003589 (RECOVER); the National Institutes of Health (no. U01 GM087719); the Open Fund of Key Laboratory of Urban Land Resources Monitoring and Simulation, Ministry of Land and Resources, China (no. KF-2019-04-034); the National Natural Science Foundation of China (nos. 61773091, 11875005, 61976025, and 11975025); and a University of Cambridge COVID-19 Rapid Response Grant. S.T.A. acknowledges

the research computing facilities and advisory services offered by Information Technology Services, The University of Hong Kong. L.W. acknowledges the computational and storage services provided by the IT department at the Institut Pasteur. **Author contributions:** L.W., S.T.A., E.H.Y.L., and B.J.C. conceived the study, designed the statistical and modeling methods, conducted analyses, interpreted results, and wrote and revised the manuscript. X.-K.X., Z.D., and Y.W. collected and compiled data, interpreted results, and revised the manuscript. G.M.L. supervised the study, interpreted results, and revised the manuscript. **Competing interests:** B.J.C. reports honoraria from Sanofi Pasteur and Roche. The authors report no other potential conflicts of interest. **Data and materials availability:** All data and codes are available in the main text, the supplementary materials, or Zenodo (23). This work is licensed under a Creative Commons Attribution 4.0 International (CC BY 4.0) license, which permits unrestricted use, distribution, and reproduction in any medium, provided the original work is properly cited. To view a copy of this license, visit <https://creativecommons.org/licenses/by/4.0/>. This license does not apply to figures/photos/artwork or other content included in the article that is credited to a third party; obtain authorization from the rights holder before using such material.

## SUPPLEMENTARY MATERIALS

[science.sciencemag.org/content/369/6507/1106/suppl/DC1](https://science.sciencemag.org/content/369/6507/1106/suppl/DC1)  
Materials and Methods  
Figs. S1 to S14  
Tables S1 to S5  
References (31–49)  
MDAR Reproducibility Checklist

[View/request a protocol for this paper from Bio-protocol.](#)

20 May 2020; accepted 13 July 2020  
Published online 21 July 2020  
10.1126/science.abc9004





## Supplementary Materials for

### **Serial interval of SARS-CoV-2 was shortened over time by nonpharmaceutical interventions**

Sheikh Taslim Ali\*, Lin Wang\*, Eric H. Y. Lau\*, Xiao-Ke Xu, Zhanwei Du, Ye Wu, Gabriel M. Leung, Benjamin J. Cowling†

\*These authors contributed equally to this work.

†Corresponding author. Email: bcowling@hku.hk

Published 21 July 2020 on *Science* First Release  
DOI: 10.1126/science.abc9004

#### **This PDF file includes:**

Materials and Methods  
Figs. S1 to S14  
Tables S1 to S5  
References

**Other Supplementary Material for this manuscript includes the following:**  
(available at [science.sciencemag.org/cgi/content/full/science.abc9004/DC1](https://science.sciencemag.org/cgi/content/full/science.abc9004/DC1))

MDAR Reproducibility Checklist (.pdf)

## **Table of Contents**

	<b>Pages</b>
<b>1. Reconstruction of transmission pairs</b>	<b>3</b>
<b>2. Stratifications of transmission pairs</b>	<b>4</b>
<b>3. Estimation of serial interval distribution</b>	<b>5</b>
<b>4. Mechanisms underlying the observed patterns</b>	<b>5</b>
<b>5. Effect of non-pharmaceutical interventions on shortening effective serial intervals over time</b>	<b>10</b>
<b>5.1 Probabilistic model of transmission pair</b>	<b>10</b>
<b>5.2 Individual-based model for simulating serial intervals</b>	<b>13</b>
<b>5.3 Multivariable regression model</b>	<b>15</b>
<b>6. Real-time transmissibility estimated under a single stable serial interval distribution versus effective serial interval distributions</b>	<b>20</b>
<b>7. Sensitivity analyses for results validation</b>	<b>20</b>
<b>7.1 Sensitivity analysis on the length of running time windows and the probability distribution for fitting</b>	<b>21</b>
<b>7.2 Examining the uncertainty for recall bias</b>	<b>23</b>
<b>7.3 Infector-based serial interval versus transmission pair based serial interval</b>	<b>25</b>
<b>8. References</b>	<b>31</b>

## Materials and Methods

### 1. Reconstruction of transmission pairs

In mainland China, 27 provincial and 264 urban health commissions publicly posted detailed reports (in Chinese) of 9,120 confirmed COVID-19 cases online during January 15 – February 29, 2020, which comprised 72.7% of all COVID-19 cases confirmed in mainland China outside Hubei Province. The original reports were the results of contact tracing and epidemiological investigations conducted by health authorities in mainland China. Each of the original case reports provides a detailed description on the demographic information (e.g., age, sex, job, residential city), travel history (e.g., returned from Hubei, transferred at Wuhan, never travelled recently), potential contacts (e.g., close contacts, face-to-face proximity), social relationships with the contacts (e.g., familial member, classmate, colleague), and epidemiological timelines if known (e.g., potential times of infection, symptom onset, hospital visit(s), isolation, confirmation, and public disclosure). By screening all of these reported cases independently by three co-authors, we reconstructed 1,407 transmission pairs using the following protocols (31):

(1) We first identified a pair or a group of confirmed cases by the information on their close contacts or familial ties. Specifically, we used the following criteria to determine whether two cases had a transmission pair due to the existence of close contact: (i) A clear statement of the keyword “close contacts” (密切接触 in Chinese); (ii) Statements indicating the existence of face-to-face proximity or physical contacts, such as “shared a meal (聚餐 in Chinese)”, “travelled together (自驾与亲属某某同行 in Chinese)”, “worked together (一起进行工作 in Chinese)”. (2) For an identified transmission pair reported with familial relationship between two cases, we used this familial relationship to determine whether it was household or non-household transmission. Specifically, we used the immediate familial relationships (e.g., a person’s spouse,

parents, and children) as the indicator of household transmission, and all other familial relationships (e.g., a person's siblings with age  $\geq 17$ ) as well as close contacts without familial information as the indicator of non-household transmission.

(3) We then determined the infector and infectee of each transmission pair according to their travel histories and locations of exposure. When two cases were reported with a single epidemiological link (i.e., no other case involved in their transmission), they often had a straightforward transmission direction as follows: The infector had a recent travel history linked to Hubei province or a close contact with other case(s) recently visited Hubei province, whereas although reported with no recent travel history to Hubei province, the infectee had a close contact with the infector and no close contacts with people returned from other provinces. When a case had several possible infectors after evaluating their travel histories and exposure locations, we assumed that the infector of this transmission pair was the one who first developed symptom. Such situation was observed for some household transmissions. For example, given three confirmed cases  $i, j$ , and  $k$  from the same household outside Hubei province and only two family members  $i$  and  $j$  recently visited Hubei, case  $k$  could be infected by either case  $i$  or  $j$ , which is difficult to infer if the exposure times of cases  $i$  and  $j$  were not available from their public reports. As a simplification, we chose the infector of case  $j$  as the family member ( $i$  or  $j$ ) with the earliest symptom onset. Our recent study (31) has validated the robustness of this approximation.

## **2. Stratifications of transmission pairs**

Along with the stratification by household settings(as defined in protocol 2 in above section), we also stratified transmission pairs by the isolation delay, age, or sex.. Denote the *isolation delay* as the time duration from the symptom onset to isolation time for the infector of each transmission



pair. The *shorter (longer) isolation delay* is used to find the transmission pairs with isolation delays shorter (longer) than the median isolation delay across those transmission pairs that are identified by a given stratification condition (e.g., household transmission). The *younger-age (older-age)* are used to find the transmission pairs with infectors younger (older) than the median age across all infectors of those transmission pairs that are identified with a given condition (e.g., household transmission). The indicator *male* and *female* are defined similarly.

### **3. Estimation of serial interval distribution**

Given a reconstructed transmission pair, the serial interval was computed as the number of days between the reported symptom onset date of the infector and of the infectee. Serial interval distribution was estimated by fitting a normal (or Gumbel) distribution to the corresponding data via Markov Chain Monte Carlo (MCMC) with Gibbs sampling and non-informative flat prior. Normal distribution is a representative of symmetric distribution, and Gumbel distribution is a representative of asymmetric distribution. To fit a normal distribution, we estimated the mean and standard deviation of the normal distribution; to fit a Gumbel distribution, we estimated the location and scale parameters of the Gumbel distribution. We confirmed the convergence of MCMC chains via trace plot and diagnosis. We obtained the posterior distribution of parameters by running 100,000 iterations with a burn-in of 40,000 iterations and a thinning interval of 10.

### **4. Mechanisms underlying the observed patterns**

From the view of a single transmission pair, the serial interval depends on the infectiousness profile of the infector and the incubation period of the infectee. On the other hand, from the view of each infector, the realized serial intervals may not only depend on the properties of each

transmission pair (i.e., infectiousness profile, incubation period) but may also depend on the properties of contacts (e.g., contact patterns (22, 32), structure of contacts (33, 34). Fig. S1 (A) illustrates the effect of these basic factors on shaping serial interval distribution.

The influence of non-pharmaceutical interventions (NPIs) on re-shaping serial interval distribution can be understood from two aspects (Fig. S1 (B)-(C)). On one hand, the implementation of NPIs via enhanced contact tracing and scaling up testing capacities reduced the time delay in isolating cases (Fig. S2), which reduces the period of infectiousness and hence truncates the exposure window for susceptible individuals to acquire infection. On the other hand, the NPI-induced truncation on the period of infectiousness may also reduce or even avoid the generation of some secondary cases, skewing the serial interval distribution to the left.

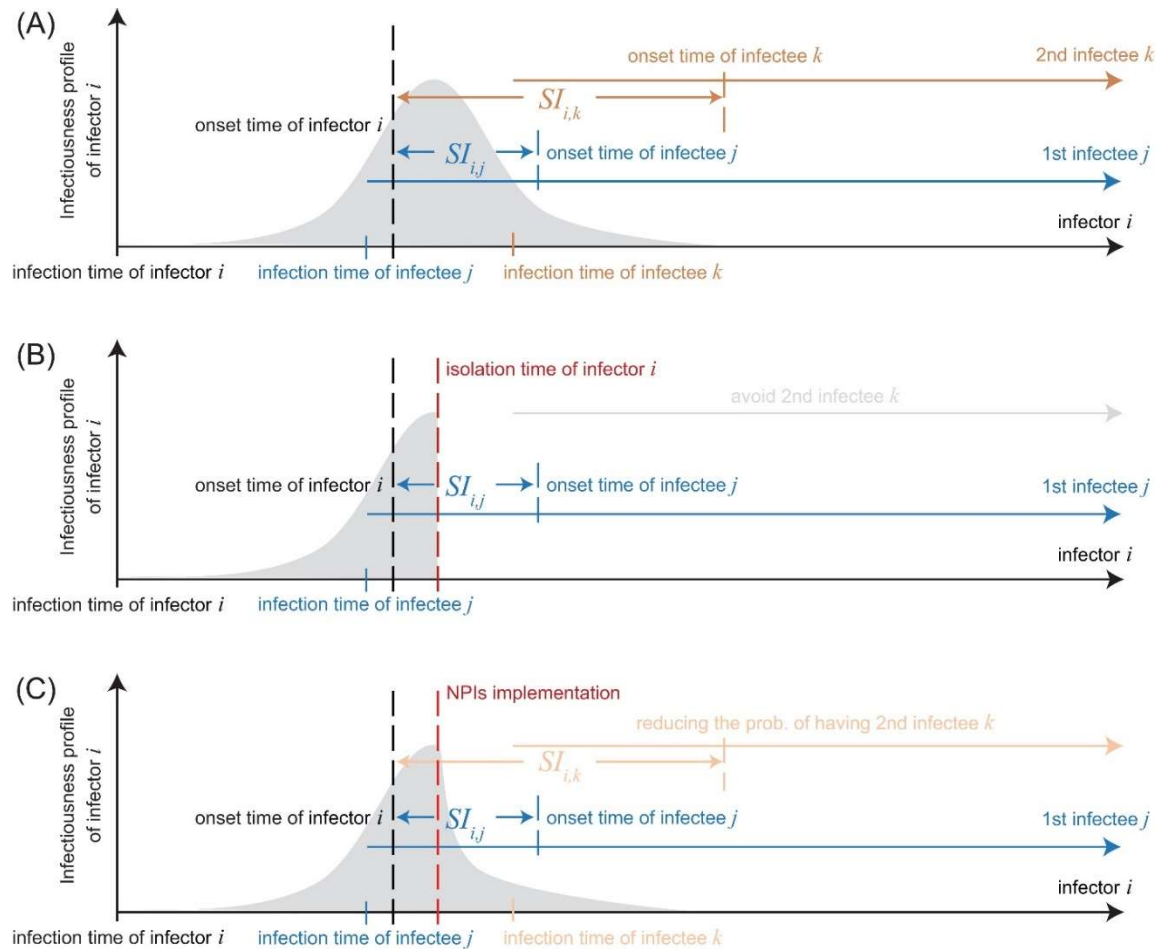


**Fig. S1:** Illustration for the influence of non-pharmaceutical intervals (NPIs) on changing serial interval distribution. (A) Without NPIs, the distribution of serial intervals depends on the properties of contacts (e.g., contact patterns, structure of contacts) and properties of transmission pair (e.g., infectiousness profile, incubation period). (B) Rapid case identification and isolation can abruptly truncate the infectiousness profile of an infector, avoiding the generation of some secondary cases thereon. (C) Other NPIs (e.g., lockdown, confinement, travel restrictions) may reduce overall infectiousness but some were triggered by symptoms and hence have a larger effect on infectiousness after symptom onset. The overall effect narrows the infectiousness profile of an infector, lowering the probability in generating secondary cases.

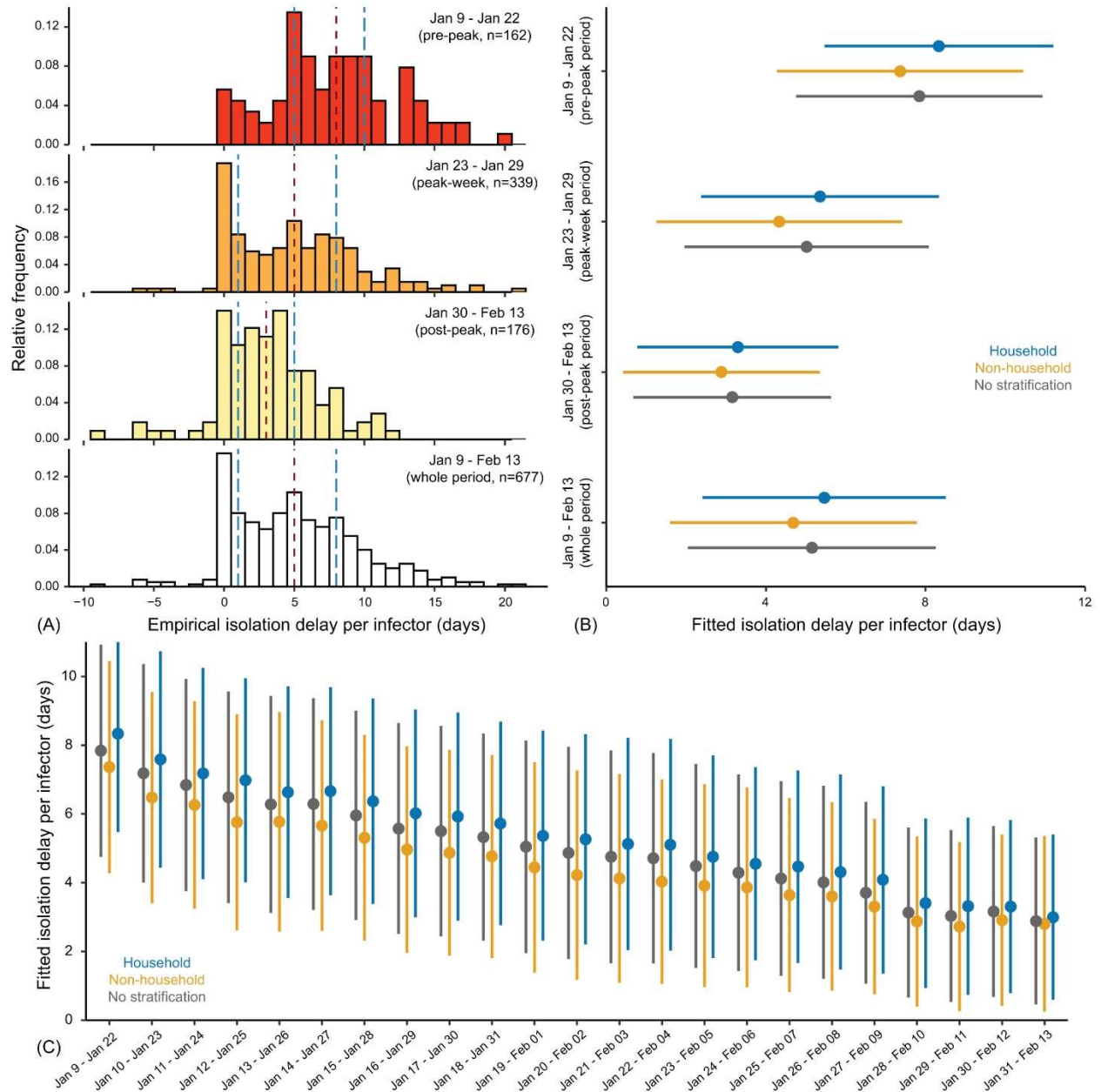


**Fig. S2:** Temporal change of the time delay in isolating COVID-19 infectors from their symptom onset (i.e., isolation delay) in mainland China. (A) Empirical isolation delay distributions. From top to bottom, transmission pairs were analyzed by selecting infectors who developed symptoms during January 9 – 22, 2020 (pre-peak), January 23 – 29, 2020 (peak-week), January 30 – February 13, 2020 (post-peak), and January 9 – February 13, 2020 (whole period), respectively. In each panel, vertical dashed lines in red and blue colors indicate the median and interquartile range (IQR). (B) Estimated isolation delay distributions by fitting a normal distribution to isolation delay data via MCMC. From top to bottom, each group of bars correspond to the transmission pairs with infectors who developed symptom during the pre-peak, peak-week, post-

peak, and whole 36-day period, respectively. Colored dots and bars correspond to the transmission pairs within households (blue), outside households (yellow), and transmission pairs with no stratification (dark-grey). (C) Estimated isolation delay distribution for each running time window by fitting a normal distribution. Dark-grey color indicates fitting data with no stratification, whereas blue (yellow) indicates fitting household (non-household) data. Dots and bars in (B) and (C) indicate the estimated median and IQR, respectively.

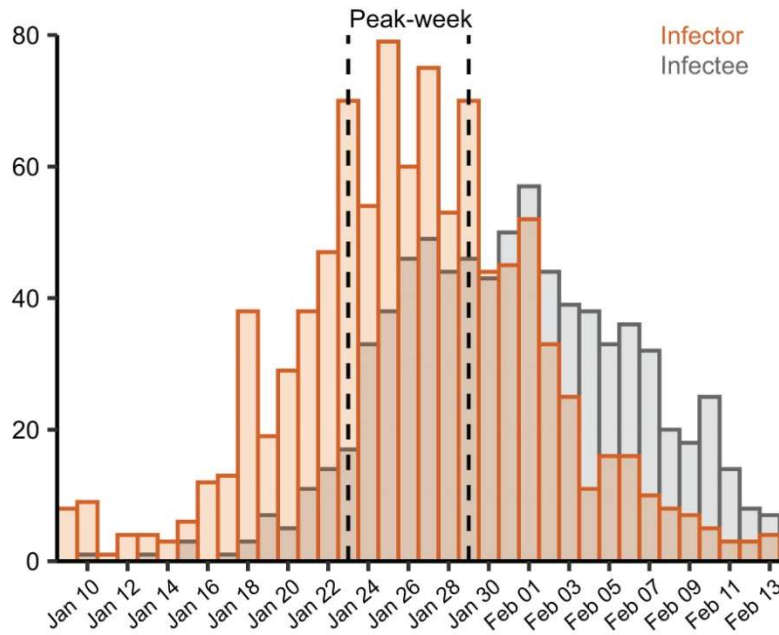


**Fig. S3:** Daily number of COVID-19 infectors (orange bar) and infectees (grey bar) by their symptom onset in China outside Hubei province during January 9 – February 13, 2020. The 1-week period during January 23 – 29, 2020, is regarded as the peak-week period, because a large number of infectors (339, ~50% of data) developed symptom during this week. The earlier 14-day period (January 9–22, 2020) is regarded as the pre-peak period, and the later 15-day period (January 30 – February 13, 2020) is regarded as the post-peak period.

## 5. Effect of non-pharmaceutical interventions on shortening effective serial intervals over time

This section tests the hypotheses (illustrated in the above section and Fig. S1) for the effect of NPIs on shortening serial intervals over time, by using a probabilistic model (section 5.1), individual-based simulations (section 5.2) and regression models (section 5.3)

### 5.1 Probabilistic model of transmission pair

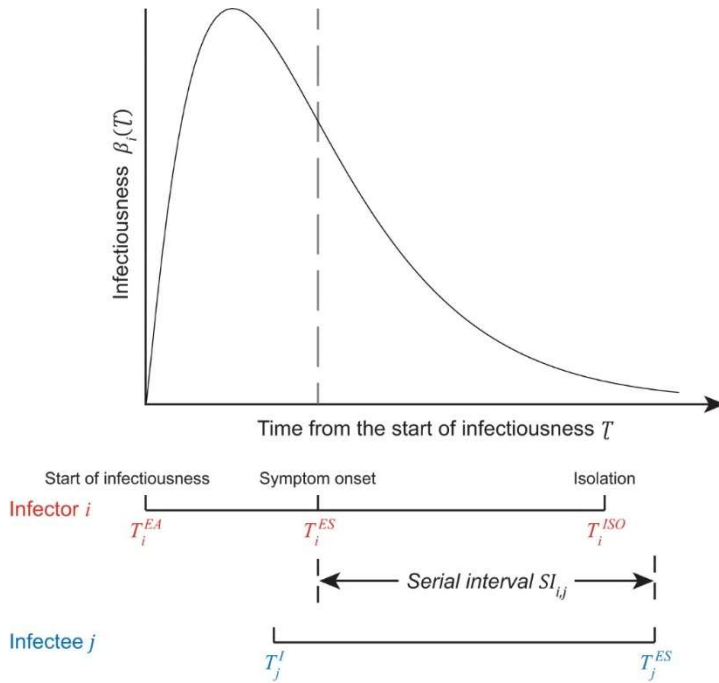


Fig. S4. Schematic of a transmission pair. The infector  $i$  starts to be infectious and symptomatic, and then is isolated at time  $T_i^{EA}$ ,  $T_i^{ES}$ , and  $T_i^{ISO}$ , respectively. The infectee  $j$  is infected by the infector  $i$  at time  $T_j^I$  and becomes symptomatic at time  $T_j^{ES}$ . Top panel illustrates the infectiousness profile of infector  $i$ , which is assumed to follow a gamma distribution.

Given a transmission pair in which the infectee  $j$  is infected by the infector  $i$  at time  $T_j^I$ , the serial interval denotes the time duration between the symptom onset time of infector  $T_i^{ES}$  and symptom onset time of infectee  $T_j^{ES}$ :  $SI_{i,j} = T_j^{ES} - T_i^{ES}$ .

Denote  $T_i^{EA}$  as the time at which the infector  $i$  starts to be infectious,  $T_i^{ISO}$  the time at which the infector  $i$  is isolated, and  $D_i = T_i^{ISO} - T_i^{ES}$  the time delay from symptom onset to isolation of infector  $i$ , respectively. We term  $D_i$  as the isolation delay.

Following He et al. (20), we define the infectiousness of infector  $i$  as the probability to infect an infectee  $\tau = T_j^I - T_i^{EA}$  days after infector  $i$  starts to be infectious at time  $T_i^{EA}$ . The probability density function (pdf) of infectiousness is assumed to follow a gamma distribution (20):  $\beta_i(\tau) = \frac{1}{\Gamma(k) \cdot \theta^k} \cdot \tau^{k-1} \cdot \exp\left(-\frac{\tau}{\theta}\right)$ , where  $k$  and  $\theta$  are the shape and scale parameters, respectively. Recent clinical (35-37), epidemiologic (16, 20, 38-40), and biological studies (41-43) suggest that the SARS-CoV-2 infection is able to shed virus particles before symptom onset, which can cause a substantial proportion of pre-symptom transmissions. Hence we consider that the infectiousness starts from  $C_i$  days before symptom onset of infector  $i$ , i.e.,  $C_i = T_i^{ES} - T_i^{EA}$ . Based on these settings, the expression of serial interval becomes:

$$SI_{i,j} = E_j^S + \tau - C_i$$

where the first term  $E_j^S = T_j^{ES} - T_j^I$  is the incubation period of infectee  $j$ . Based on the detailed exposure history for the first 425 confirmed SARS-CoV-2 cases in Wuhan, Li et al. (17) suggested that the pdf of incubation period  $P(E^S)$  follows a log-normal distribution with a mean of 5.22 days and standard deviation of 3.87 days.

Given an isolation delay  $D_i$  that is assumed to occur before symptom onset of infectee, the pdf of serial intervals is obtained by integrating over the range of time interval  $\tau$ :



$$P(SI_{i,j}) = \int_0^{C_i+D_i} \beta_i(\tau) \cdot P(E^S = SI_{i,j} + C_i - \tau) d\tau$$

The cumulative distribution is given by  $\int_{-\infty}^x P(SI_{i,j}) dSI_{i,j}$ , and the mean serial interval is given by:  $\int_{-\infty}^{\infty} SI_{i,j} P(SI_{i,j}) dSI_{i,j}$ .

To compare with data of transmission pairs in which serial interval and isolation delay were available, we also computed the pdf of serial intervals with minimum isolation delay  $D_i^{min}$ :

$$P(SI_{i,j}, D_i^{min}) = \int_{D_i^{min}}^{\infty} P(D_i) \int_0^{C_i+D_i} \beta_i(\tau) \cdot P(E^S = SI_{i,j} + C_i - \tau) d\tau dD_i$$

where  $P(D_i)$  is the distribution of isolation delay  $D_i$ , which can be obtained by fitting isolation delay data.

We parameterized the start time of infectiousness  $C_i$ , and the shape  $k$  and scale  $\theta$  of the gamma distribution of infectiousness with inferred results by He, X. et al. (20). We tested the following three scenarios which were selected from the high likelihood region estimated by He, X. et al. (20).

Parameters	Scenario-I	Scenario-II	Scenario-III
$C_i$	2 days	4 days	6 days
Shape $k$	2.15	2.74	1.53
Scale $\theta$	1.34	1.71	4.38

This simple model suggests that serial intervals become shorter the faster the infectors are isolated, regardless of when an infector starts to be infectious before illness onset (fig S5).

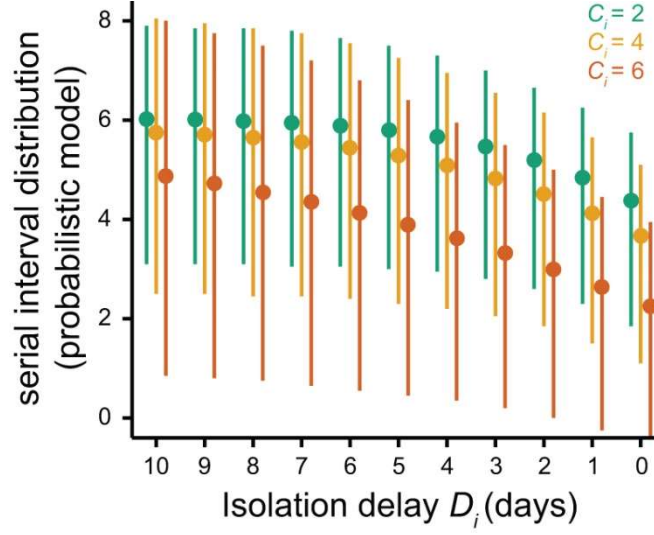


**Fig. S5.** Using probabilistic model to examine the effect of non-pharmaceutical interventions (NPIs) on shortening serial intervals over time. Serial intervals are estimated with the probabilistic model based on a transmission pair, in which the start time of infectiousness  $C_i$  is considered as 2 (green), 4 (yellow), or 6 (orange) days before symptom onset of infector. Given each isolation delay  $D_i$ , the dot and vertical bar indicate the mean and interquartile range (IQR) of estimated distribution.

## 5.2 Individual-based model for simulating serial intervals

We also simulated the serial intervals by using an individual-based model. Specifically, we started with a number of cases who have been infected at the time origin. Each potential infector will infect a number of infectees, which follows a Poisson distribution with mean  $R_e$ , the effective reproduction number. The exact infection times will be simulated according to the generation time. However, knowledge on the generation time for COVID-19 is still limited, and hence was approximated by published serial intervals, with a gamma distribution and a mean of 5.1 days (27), which is the same as our estimates during the peak-week period for COVID-19 in mainland China. In other scenarios, we assumed shorter and longer serial intervals respectively, which were the same as that estimated with means of 7.8 (as estimated from the pre-peak

period), 2.6 (as estimated from the post-peak period) and 8.4 days (as estimated for the 2003 SARS epidemic (44)). From the simulated infection times, we added the simulated incubation period for all infectees, assuming a lognormal distribution with mean 5.2 days (17). The duration between the symptom onset times of the infector and infectee in each transmission pair would be the simulated serial intervals. We present the mean serial intervals and their 95% confidence intervals from 500 transmission pairs in 200 simulations under different initial effective reproduction number  $R_e$  (e.g. 3.0, 2.5, 2.0, 1.5, 1.0, 0.5, 0.3) (25) to represent situations with different level of general control measures (e.g. social distancing, enhanced personal hygiene) in place, and reducing time delay from symptom onset to isolation (e.g. from 10 to 0 days) which was assumed to interrupt further transmission after a case has been isolated.

The results from individual-based simulations suggest the possible association between serial interval and isolation delay (Fig. S6, Table S4). Given a mean generation time of 7.8 days (as per our estimate for the pre-peak period of COVID-19 in mainland China), the simulated mean serial intervals reduces from ~8.0 to ~1.2 days when the isolation delay reduces from 10 to 0 days. Given a mean generation time of 5.1 days (as per our estimate for the peak-week period of COVID-19 in mainland China, which is similar to the estimates by Zhang *et. al.* (27)), the simulated mean serial interval reduces from ~5.1 to ~1.5 days when the isolation delay reduces from 10 to 0 days. Similar outcomes were obtained with alternative generation times with a mean of 2.6 days (estimate for the post-peak period) and 8.4 days (as estimated for the 2003 SARS epidemic (44)) (Table S4). The temporal change of serial intervals is less sensitive to the variation in initial effective reproduction number,  $R_e$  (a measure of initial transmission

accounting for the effect of control measures). Our analytical and simulated models validate that serial interval is positively associated with isolation delay.

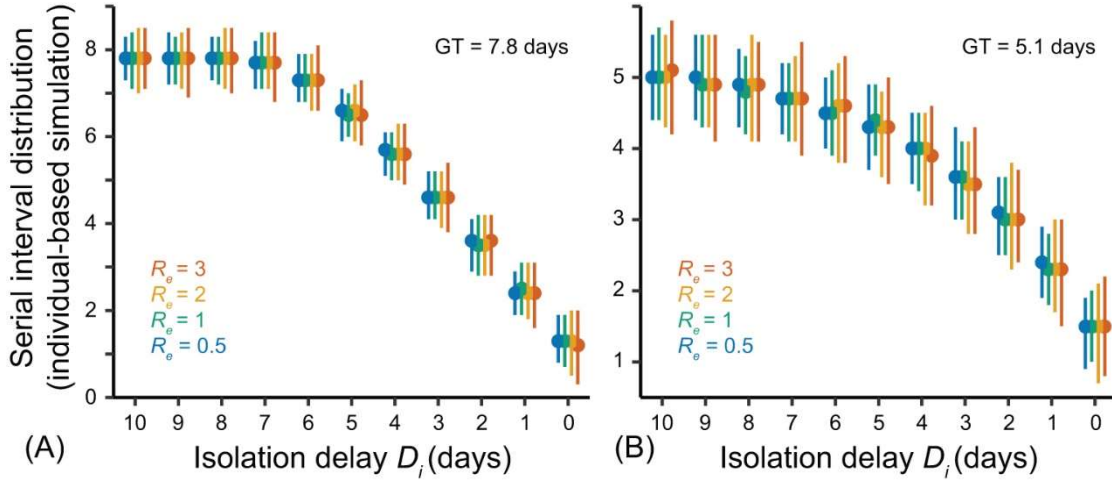


**Fig. S6.** Using individual-based simulation model to examine the effect of non-pharmaceutical interventions (NPI) on shortening serial intervals over time. Given each combination of isolation delay  $D_i$  and initial effective reproduction number  $R_e$ , the dots and vertical bars indicate the median and IQR of estimated distribution, when the mean generation time (GT) is 7.8 days in (A) and 5.1 days in (B).

### 5.3 Multivariable regression model

Since the implementation of a cordon sanitaire around Wuhan on January 23, 2020, multiple NPI strategies have been implemented in more than 260 Chinese cities, including the isolation of confirmed and suspected cases, suspension of intra-city public transport, suspension of travel between cities, social distancing by closure of entertainment and public gathering venues (e.g., bars, cinemas and parks), as well as public services (e.g., shopping malls and restaurants), and recruitment of governmental staff and volunteers to enforce quarantine (Fig. S7). To study the influence of these factors on COVID-19 transmission, we developed a series of linear univariate

and multivariable regression models to predict empirical serial intervals with infectors that developed symptoms on each day.

We evaluated the daily time series of following measures from transmission pairs. Denote,  $\omega(t)$  and  $d(t)$  as the observed serial interval and isolation delay on day  $t$ , respectively. We calculated  $\omega(t)$  by the median of all serial intervals with infectors developed symptoms on day  $t$ , and  $d(t)$  by the median of time delay from symptom onset to isolation for infectors with symptoms during day  $t$ , who caused infectees further. To quantify the daily intensity of each NPI strategy in mainland China, we also counted the number of cities in mainland China that implemented each NPI measure on day  $t$ , using the interventions data from more than 260 Chinese cities (24) (Fig. S7). The NPI measures include the isolation of suspected and confirmed cases, travel ban for intra-city and inter-city movement, social distancing by closing public services (e.g., hospitals, shopping malls, restaurants) and entertainment venues (e.g., cinema, bar, café) and recruiting government workers and volunteers to assist quarantine and social distancing. Denote  $\eta_k(t)$  as the cumulative number of cities in mainland China that implemented the  $k$ -th intervention ( $k = 1, 2, \dots, 7$ ) on day  $t$ .

We first used univariate linear regression models to test the association between each intervention measure and daily serial interval  $\omega(t)$ , and then significant factors are included one in addition to linear multi-variable regression model to predict the daily serial interval  $\omega(t)$ :

$$\omega(t) \sim \beta_0 d(t) + \beta_k \eta_k(t), k = 1, 2, \dots, 7$$

where each  $\beta_i$  is a regression coefficient for respective factors. Because the isolation delay is expected to be a prime driver of serial intervals, we considered a baseline model as  $\omega_{base}(t) =$

$\beta_0 d(t)$ , where  $d(t)$  is the daily isolation delay (the median daily isolation delay).  $\eta_1(t)$  and  $\eta_2(t)$  are the daily cumulative number of cities implemented the isolation on suspected and confirmed cases respectively. The travel restrictions consist of  $\eta_3(t)$  and  $\eta_4(t)$ , the daily cumulative number of cities implemented the inter-city and intra-city travel ban respectively. The social distancing measures are  $\eta_5(t)$ ,  $\eta_6(t)$  and  $\eta_7(t)$ , the daily cumulative number of cities implemented the closure of public services, closure of entertainment venues, and recruitment of government workers and volunteers to assist quarantine, respectively. Finally, we estimated the contribution of each factor according to the improvement in predicting the daily serial interval  $\omega(t)$  by including each factor into the baseline model.

The univariate regression model suggests that the isolation delay is the better predictor of daily serial interval (Fig. S8). The basic regression model that only accounting for isolation delay can explain up to 51.5% of the variability in daily empirical serial interval, indicating isolation delay as the prime factor. The improved models that combine the basic model with one of either the additional factors (NPI strategy or accumulation of population immunity) can explain a further maximum of 15.6% - 16.7% variability in daily empirical serial intervals (Table S5). The model fitting further suggests a potential explanation about for how serial intervals can be modulated by respective interventions over the span of outbreak (Fig. 9). We found that, per day of early isolation, the predicted serial interval decreased by 0.7 (95% confidence interval, CI: 0.4, 0.9) days on average. Although the effects of these additional factors in combination of isolation delay are identified specifically in non-household setting, we were not able to detect their individual contribution to change serial intervals (Table S5).

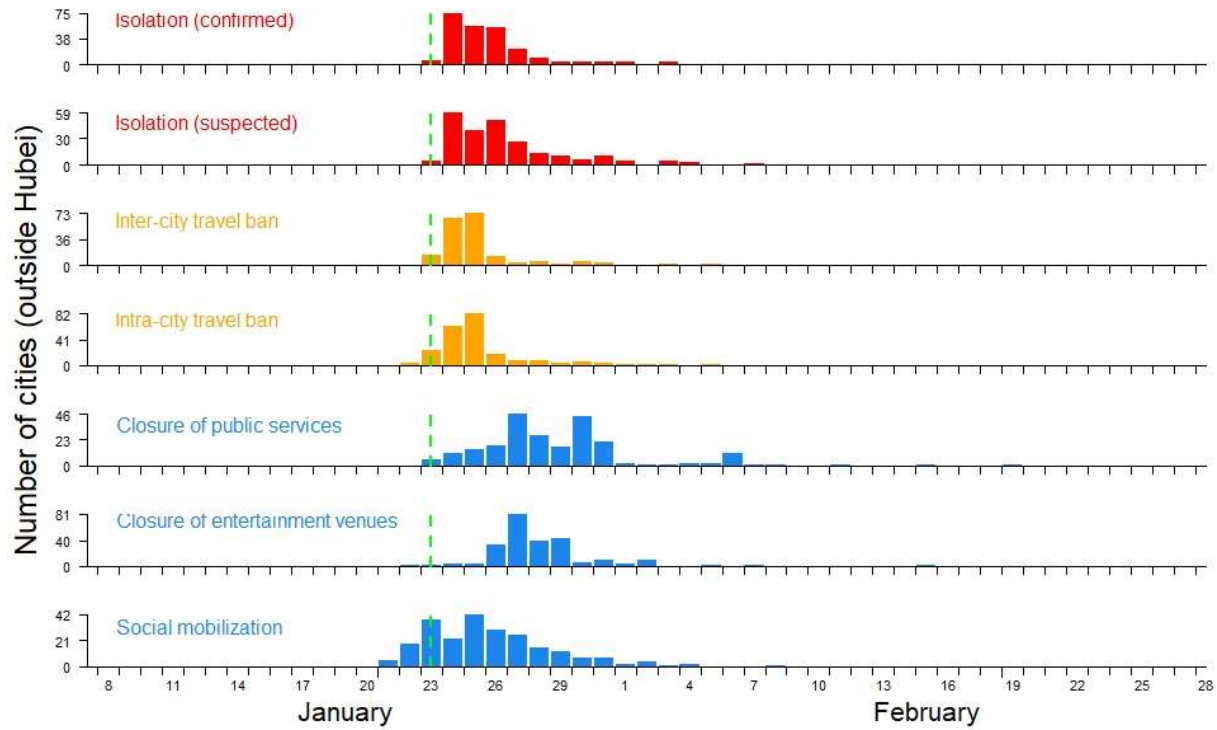


**Fig. S7:** Timelines for the number of Chinese cities (excluding cities in Hubei province) that were starting to implement each of the following 7 non-pharmaceutical interventions: isolation of confirmed cases, insolation of suspected cases, suspension of travel between cities (i.e., inter-city travel ban), suspension of intra-city public transport (intra-city travel ban), closure of public services (e.g., shopping malls, restaurants), closure of entertainment and public gathering venues (e.g., bar, cinema, park), and recruitment of governmental staff and volunteers to enforce quarantine (i.e., social mobilization).

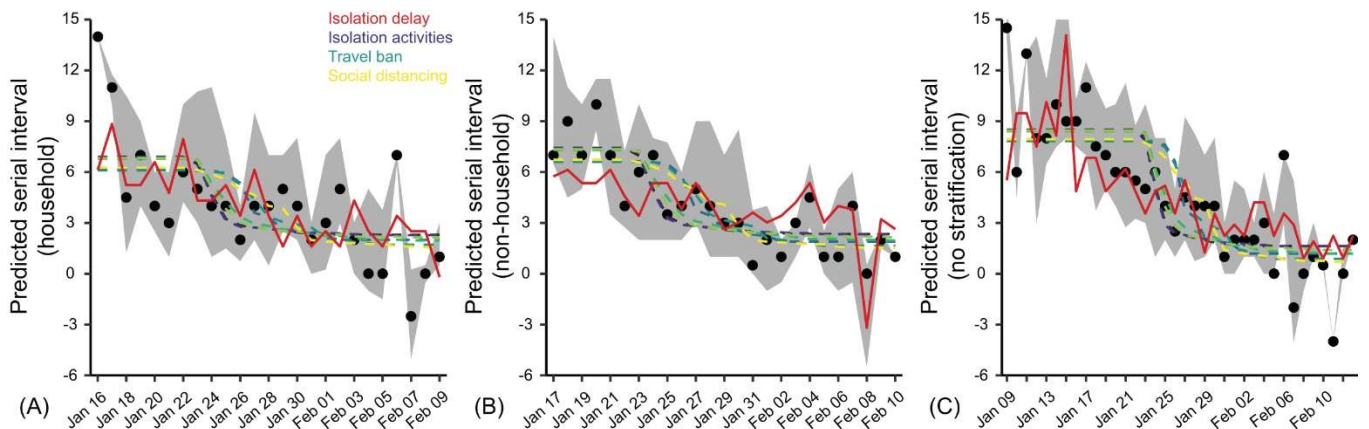




**Fig. S8.** The univariate regression models to examine the effect of non-pharmaceutical interventions (NPI) on shortening serial intervals over time. Prediction of empirical serial intervals with infectors that developed symptom on each day (by univariate regression models), for (A) household, (B) non-household, and (C) all transmission pairs. Black dots and grey shaded regions indicate the median and IQR of empirical serial intervals. Red curves indicate the mean of serial intervals predicted by isolation delay of infectors. Dashed curves in other colors indicate the mean serial intervals predicted by individual factors including isolating confirmed cases, isolating suspected cases, inter-city travel ban, intra-city travel ban, closure of public services, closure of entertainment venues and social mobilization.

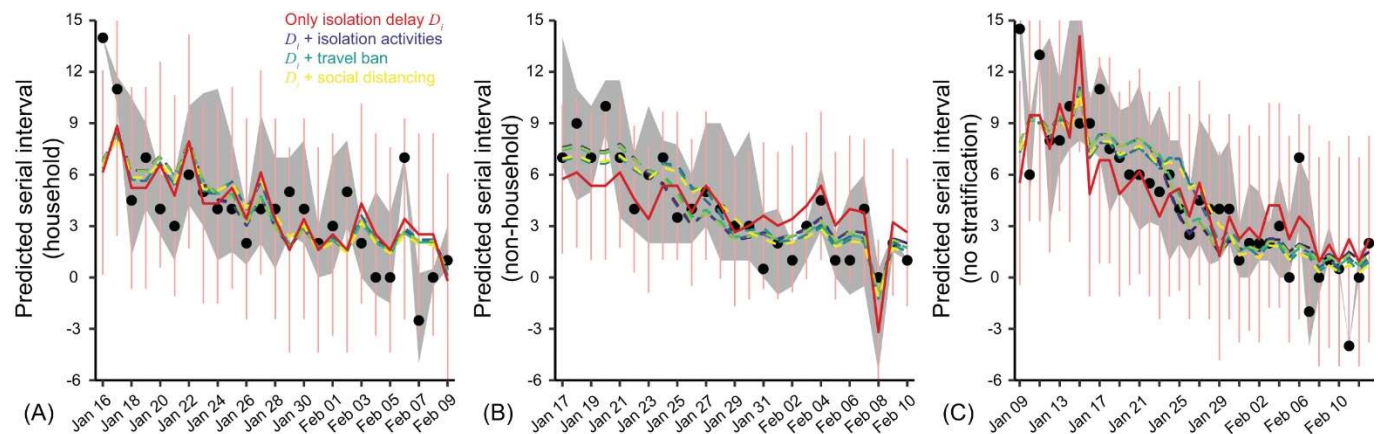


**Fig. S9.** The multi-variable regression models to examine the effect of non-pharmaceutical interventions (NPI) on shortening serial intervals over time. Prediction of empirical serial intervals with infectors that developed symptom on each day (by multivariable regression models), for (A) household, (B) non-household, and (C) all transmission pairs. Black dots and grey shaded regions indicate the median and IQR of empirical serial intervals. Red curves indicate the mean (with 95% confidence interval in light-pink vertical bars) of serial intervals predicted with the basic regression model only accounting for the isolation delay of infectors. Dashed curves in other colors indicate the mean serial intervals predicted by extending the basic regression model to further account for any one of the following factors: isolating confirmed cases, isolating suspected cases, inter-city travel ban, intra-city travel ban, closure of public services, closure of entertainment venues and social mobilization.

## 6. Real-time transmissibility estimated under a single stable serial interval distribution versus effective serial interval distributions

The real-time transmissibility of an infectious disease is often characterized by the instantaneous reproduction number ( $R_t$ ), which is defined as the expected number of secondary infections caused by an infector on day  $t$  (28, 45, 46). The pathogen spreads when  $R_t > 1$  and is under control when  $R_t < 1$ . To estimate  $R_t$ , a routine protocol is to approximate the generation time distribution with a single stable serial interval distribution. Let  $w_i$  be the serial interval distribution that approximates the infectiousness profile of an infected individual at  $i$ -th day since infection. Then, the daily estimate of  $R_t = \frac{I_t}{\sum_{i=1}^t I_{t-i} w_i}$  is calculated as the ratio between the number of cases  $I_t$  on day  $t$  and the weighted average of infectiousness caused by cases infected before day  $t$ , i.e.,  $\sum_{i=1}^t I_{t-i} w_i$  (47).

Because we considered time-varying serial interval distributions,  $R_t$  is reconstructed as  $R_t = \frac{I_t}{\sum_{i=1}^t I_{t-i} w_i(t)}$ , in which the infectiousness  $w_i(t)$  describes the probability at which individuals who are infected for  $i$  days before day  $t$  generate secondary infections at time  $t$ . We estimated the time-varying serial interval distribution using running time windows (Fig 2A). We compared daily  $R_t$  estimated with time-varying effective serial interval distributions versus with a single fixed serial interval distribution (Figs. 2B-D).

## 7. Sensitivity analyses for results validation

To validate our results, we performed following sensitivity analyses.

### **7.1. Sensitivity analysis on the length of running time windows and the probability**

**distribution for fitting** In the main text, we have used 14-day running time windows to estimate the real-time serial interval distributions. Here, we examined the effect of using shorter or longer length of running time windows. Using 7-day (Fig. S10A), 10-day (Fig. S10B), or 18-day (Fig. S10D) running time windows, we observed similar patterns of serial intervals shortened over time.

We also examined the alternative estimates of serial interval distributions by fitting a Gumbel distribution to data (Fig. S11). The Gumbel distribution is chosen as a representative of asymmetric distributions. Using other asymmetric distributions (e.g., Logistic distribution (31)) should give similar conclusions.

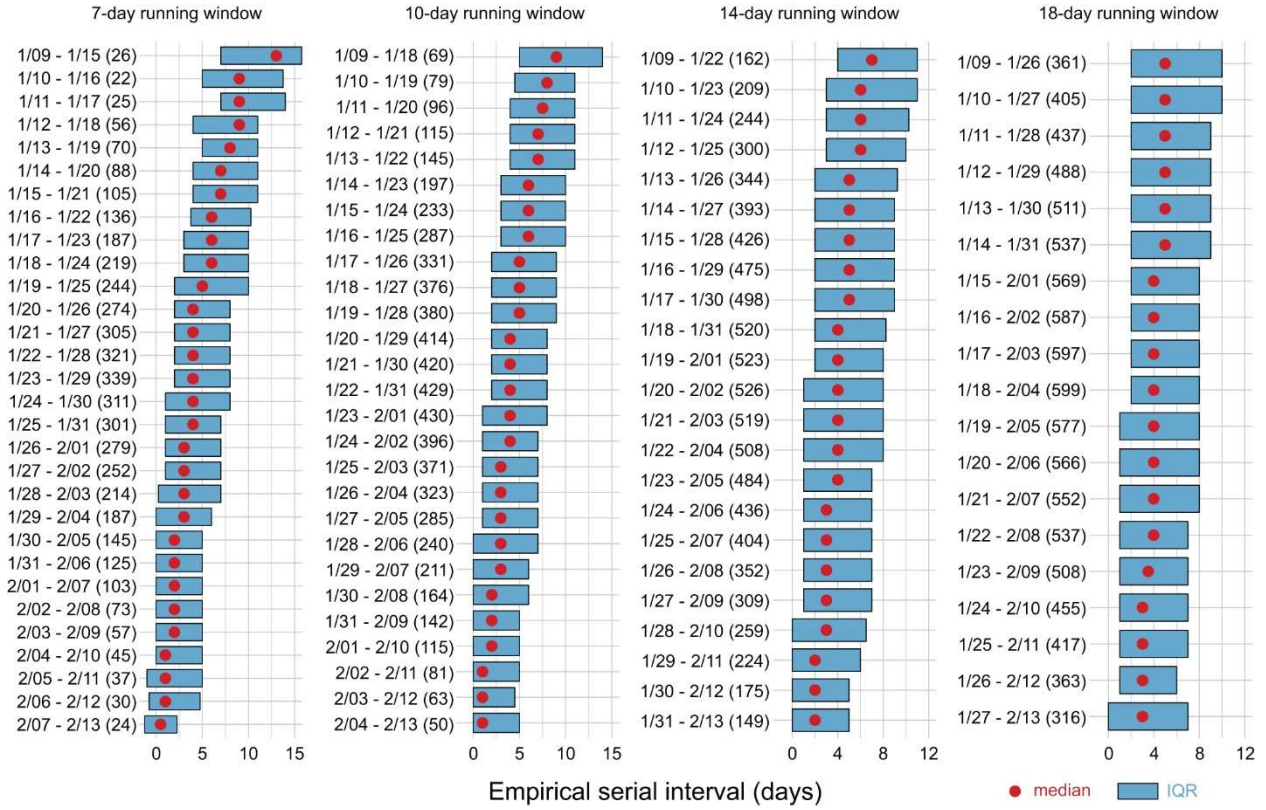


**Fig. S10:** Empirical distributions of serial interval data in each running time window shifting from January 9 to February 13, 2020. From left to right, each column corresponds to the use of (A) 7-day, (B) 10-day, (C) 14-day, and (D) 18-day running windows, respectively. In each row of each column, the dates and the number on the left-hand side indicate the specific duration and sample size  $n$  of that time window, and the red dot and blue bar indicate the median and interquartile range (IQR) of serial interval data in that time window, respectively.

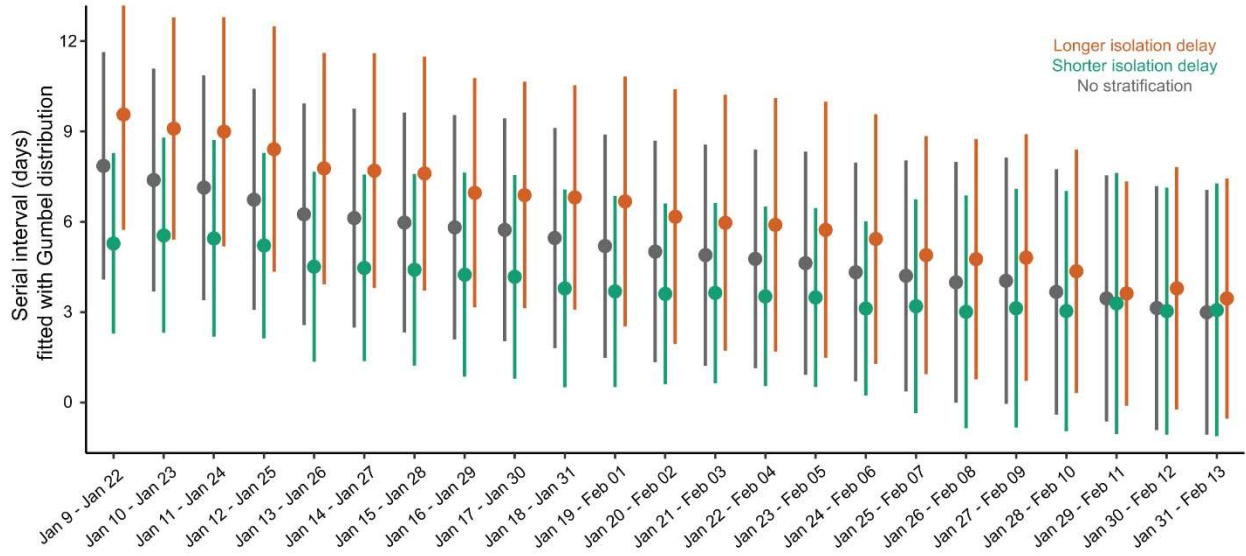


**Fig. S11:** Serial interval distribution estimated for each of the 14-day running time windows. The first running time window contains the transmission pairs with symptom onset of infectors during January 9 – 22, 2020; the second window contains the transmission pairs with symptom onset of infectors during January 10 – 23, 2020; and so on. Posterior samplers were obtained by fitting a Gumbel distribution to the serial interval data in each time window via MCMC. Dots and bars indicate the median and interquartile range (IQR) for the estimated distribution, respectively. Dark-grey color indicates the fitting for serial interval data with no stratification. Green (orange) indicates the fitting for the data with isolation delay shorter (longer) than the median isolation delay of each running time window.

## 7.2. Examining the uncertainty in recall bias

The centralized response in mainland China was established by the command system by which the State Council can coordinate a multi-sectoral joint response to promptly mobilize and deploy necessary resources (48, 49). Despite this, recall bias may be encountered when suspected or confirmed cases were checking for infection history and epidemiological timelines (e.g. symptom onset dates). As such, we performed a sensitivity analysis to account for the uncertainty in recalling symptom onset date for each case. For example, given a case who developed symptom on day  $T$  and a recall bias of  $\tau$  days, we randomly sampled the onset date of this case between  $T - \tau$  and  $T + \tau$ . We tested the effect of recall bias by using  $\tau = 1, 2$ , or 4 days. This sensitivity analysis validates the robustness of our results (Figs. S12, S13).

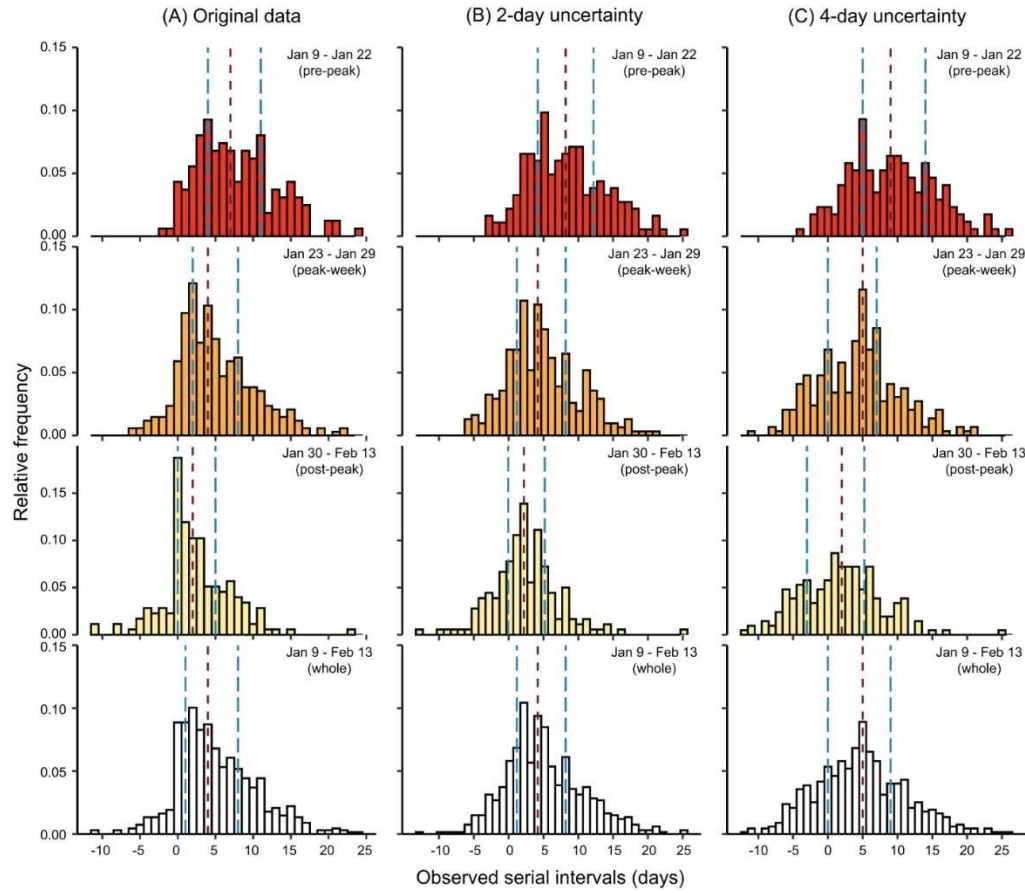


**Fig. S12:** Sensitivity analysis of empirical serial interval distributions by accounting for uncertainty in recall bias. Left column (A) shows original results without resampling of recall bias. Middle and right columns show the results obtained by resampling the onset date of each case with a recall bias of  $\tau = 2$  days (B) and  $\tau = 4$  days (C), respectively. In each column, from top to bottom, the transmission pairs were analyzed by selecting infectors who developed symptom during January 9 – 22, 2020 (pre-peak), January 23 – 29, 2020 (peak-week), January 30 – February 13, 2020 (post-peak), and January 9 – February 13, 2020 (whole period), respectively. In each panel, vertical dashed lines in red and blue colors indicate the median and interquartile range (IQR).

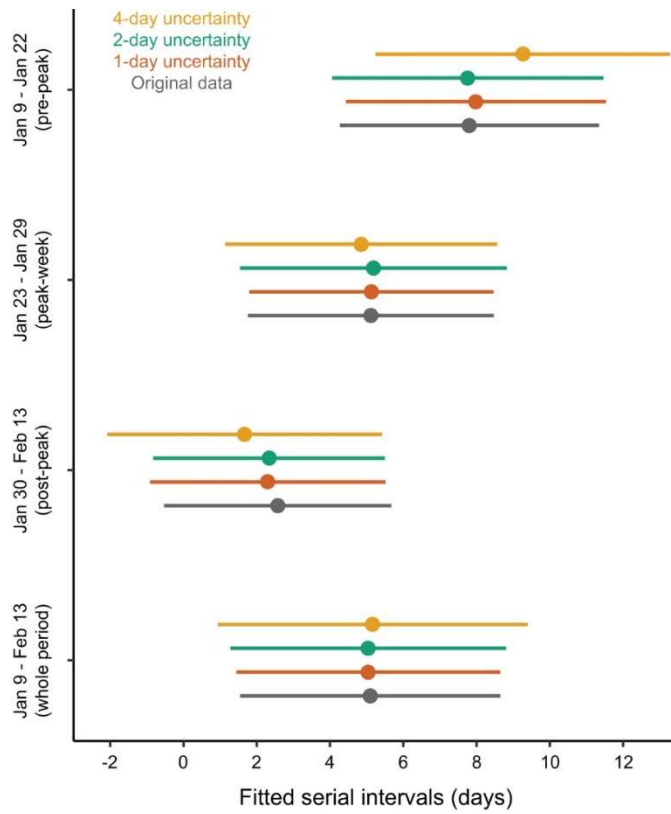


**Fig. S13:** Sensitivity analysis of the estimated serial interval distributions by accounting for uncertainty in recall bias. Serial interval distribution is estimated by fitting a normal distribution via MCMC. From top to bottom, each group of bars correspond to the transmission pairs with infectors who developed symptom during the pre-peak, peak-week, post-peak, and whole 36-day period, respectively. Dark-grey color shows original results without resampling of recall bias. Other colors show the results obtained by resampling the onset date of each case with a recall bias of  $\tau = 1$  day (orange),  $\tau = 2$  days (green), and  $\tau = 4$  days (yellow), respectively. Dots and bars indicate the estimated median and interquartile range (IQR).

### 7.3. Infector-based serial interval versus transmission pair based serial interval

In our main analysis, the serial interval distributions are calculated in terms of infector-infectee pairs. It is also worth testing the serial interval distribution as the distribution of mean serial interval per infector. If there is significant correlation between the number of infectees and the isolation delay as per infector, then serial interval distribution based on infectors would be



different from that based on transmission pairs. Fig. S14 shows the distribution of mean serial interval per infector for non-overlapping periods. Compared Fig. S14 to Fig. 1, the infector-based calculation of serial intervals is essentially the same as the transmission pair based calculation of serial intervals.

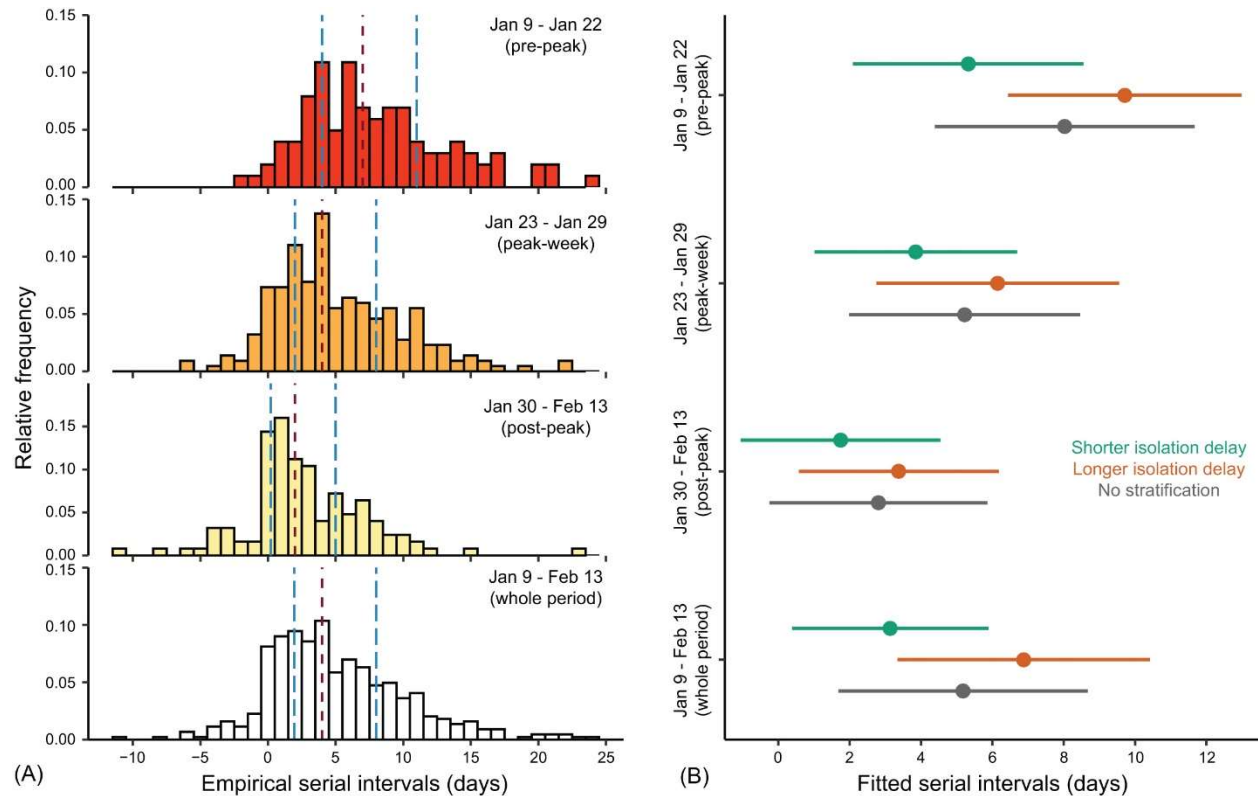


**Fig. S14:** Temporal change for infector-based serial intervals of COVID-19 in mainland China. (A) Empirical serial interval distributions. From top to bottom, transmission pairs were analyzed by selecting infectors who developed symptom during January 9 – 22, 2020 (pre-peak), January 23 – 29, 2020 (peak-week), January 30 – February 13, 2020 (post-peak), and January 9 – February 13, 2020 (whole period), respectively. In each panel, vertical dashed lines in red and blue colors indicate the median and interquartile range (IQR). (B) Estimated serial interval distributions by fitting a normal distribution via MCMC. From top to bottom, each group of bars correspond to the transmission pairs with infectors who developed symptom during the pre-peak, peak-week, post-peak, and whole 36-day period, respectively. Colored dots and bars correspond to the infectors with isolation delay shorter than the median isolation delay of each period (green), and with isolation delay longer than the median isolation delay of each period (orange), respectively. Dark-grey bars correspond to transmission pairs with no stratification.

**Table S1: Entire dataset of 1,407 transmission pairs in mainland China is available at our GitHub: [https://github.com/PDGLin/COVID19\\_EffSerialInterval\\_NPI\(23\)](https://github.com/PDGLin/COVID19_EffSerialInterval_NPI(23)).**

**Table S2:** Estimated mean and standard deviation (sd) of serial intervals. The columns entitled “Pre-peak period”, “Peak-week period”, “Post-peak period”, and “Whole period” correspond to fitting transmission pair data with infectors developed symptom during the pre-peak period (January 9 – 22, 2020), peak-week period (January 23 – 29, 2020), post-peak period (January 30 – February 13, 2020), and the whole 36-day period (January 9 – February 13, 2020). Each cell in this table presents the estimated median and 95% CrI. Model fitting is performed by fitting a normal distribution via MCMC. Fitting with alternative distributions (e.g., Gumbel distribution) gives similar estimates.

Factors	Pre-peak period			Peak-week period			Post-peak period			Whole period		
	Mean	sd	n	Mean	sd	n	Mean	sd	n	Mean	sd	n
<b>Household</b>	7.2 (5.9, 8.5)	5.4 (4.6, 6.5)	69	5.2 (4.5, 6.0)	5.1 (4.6, 5.7)	175	3.0 (2.0, 3.9)	4.7 (4.1, 5.5)	94	5.0 (4.4, 5.6)	5.2 (4.9, 5.7)	338
<b>Non-household</b>	8.3 (7.2, 9.3)	5.1 (4.5, 6.0)	93	5.0 (4.2, 5.7)	4.9 (4.4, 5.5)	164	2.1 (1.1, 3.1)	4.5 (3.9, 5.3)	82	5.2 (4.6, 5.8)	5.3 (4.9, 5.7)	339
<b>Shorter isolation</b>	5.3 (4.1, 6.4)	4.4 (3.7, 5.4)	60	4.1 (3.3, 4.9)	4.7 (4.2, 5.3)	140	1.6 (0.7, 2.5)	3.9 (3.4, 4.7)	77	3.3 (2.8, 3.8)	4.5 (4.1, 4.9)	292
<b>Longer isolation</b>	9.4 (8.3, 10.4)	5.0 (4.3, 5.8)	91	6.0 (5.2, 6.8)	5.2 (4.7, 5.8)	168	3.4 (2.4, 4.4)	4.6 (4.0, 5.4)	80	6.8 (6.2, 7.3)	5.3 (4.9, 5.7)	324
<b>Younger age</b>	7.4 (6.3, 8.5)	4.9 (4.2, 5.8)	77	5.0 (4.3, 5.8)	4.8 (4.3, 5.4)	159	3.2 (2.0, 4.3)	5.1 (4.4, 6.0)	80	5.1 (4.6, 5.7)	5.1 (4.7, 5.5)	316
<b>Older age</b>	8.8 (7.4, 10.0)	5.6 (4.8, 6.6)	74	5.2 (4.5, 6.0)	5.2 (4.7, 5.8)	175	2.1 (1.3, 3.0)	4.2 (3.7, 4.9)	94	5.1 (4.5, 5.7)	5.5 (5.1, 5.9)	343
<b>Male</b>	7.9 (6.9, 9.0)	5.3 (4.6, 6.1)	101	5.1 (4.4, 5.8)	5.3 (4.8, 5.8)	203	2.4 (1.5, 3.2)	4.5 (3.9, 5.1)	114	5.0 (4.5, 5.6)	5.4 (5.1, 5.8)	418
<b>Female</b>	7.8 (6.5, 9.2)	5.2 (4.3, 6.3)	59	5.1 (4.3, 5.9)	4.6 (4.1, 5.2)	133	3.0 (1.7, 4.2)	4.9 (4.1, 5.9)	62	5.2 (4.6, 5.9)	5.0 (4.6, 5.5)	254
<b>All pairs</b>	7.8 (7.0, 8.6)	5.2 (4.7, 5.9)	162	5.1 (4.6, 5.7)	5.0 (4.6, 5.4)	339	2.6 (1.9, 3.2)	4.6 (4.2, 5.1)	176	5.1 (4.7, 5.5)	5.3 (5.0, 5.6)	677

Note: SI=Serial interval, sd= Standard deviation, n=size of the transmission pairs

**Table S3:** Estimated mean serial intervals for transmission pairs with infectors developed symptom during the early period (first 14-day running time window during January 9 – 22, 2020) and the end period (last 14-day running time window during January 31 – February 13, 2020). Transmission pairs are stratified by different factors (i.e., isolation delay, age, or gender) and settings (i.e., household, non-household, or all transmission pairs). Each cell in this table presents the estimated median and 95% CrI. Model fitting is performed by fitting a normal distribution to the serial interval data truncated by a 14-day time window. Fitting with alternative distributions (e.g., Gumbel distribution) gives similar estimates.

Factors		Household		Non-household		All pairs	
		Early period	End period	Early period	End period	Early period	End period
Isolation delay	Shorter isolation	4.9 (3.1, 6.7)	1.9 (0.5, 3.5)	6.1 (4.5, 7.8)	0.7 (0.0, 2.0)	5.3 (4.1, 6.4)	1.4 (0.5, 2.3)
	Longer isolation	8.9 (7.1, 10.6)	3.1 (1.7, 4.5)	9.6 (8.2, 11.0)	2.6 (1.0, 4.1)	9.4 (8.3, 10.4)	3.0 (1.9, 4.1)
Age	Younger age	6.6 (5.2, 8.1)	3.1 (1.2, 5.0)	8.0 (6.3, 9.6)	2.7 (1.2, 4.3)	7.4 (6.4, 8.6)	2.9 (1.7, 4.1)
	Older age	8.2 (5.8, 10.4)	2.2 (1.0, 3.3)	9.2 (7.7, 10.7)	1.0 (0.1, 2.4)	8.7 (7.5, 10.0)	1.6 (0.7, 2.5)
Gender	Male	7.1 (5.4, 8.8)	1.7 (0.5, 2.9)	8.5 (7.2, 9.8)	2.1 (0.7, 3.5)	7.9 (6.9, 9.0)	1.9 (0.9, 2.8)
	Female	7.6 (5.4, 9.7)	4.7 (2.5, 6.9)	8.1 (6.3, 9.9)	1.5 (0.2, 3.0)	7.8 (6.5, 9.2)	2.8 (1.5, 4.1)
All above factors		7.2 (5.9, 8.5)	2.6 (1.5, 3.6)	8.3 (7.2, 9.3)	1.8 (0.7, 2.8)	7.8 (7.0, 8.6)	2.2 (1.5, 2.9)

**Table S4:** Estimated mean serial intervals (with the 95% CI in brackets) from the simulated scenarios under different combinations of isolation delay and initial effective reproduction number  $R_e$ . We approximated the generation time by serial interval distribution with a mean of 2.6 days in scenario-I, 5.1 days in scenario-II, 7.8 days in scenario-III and 8.4 days in scenario-IV.

Simulated serial intervals (Scenario-I: generation time approximated by serial intervals with mean 2.6 days)							
Isolation delay (d)	$R_e=3.0$	$R_e=2.5$	$R_e=2.0$	$R_e=1.5$	$R_e=1.0$	$R_e=0.5$	$R_e=0.3$
0	1.6 (0.7, 2.3)	1.5 (0.8, 2.2)	1.6 (0.9, 2.2)	1.6 (1.0, 2.0)	1.5 (0.9, 2.1)	1.6 (1.1, 2.1)	1.5 (1.0, 2.0)
1	2.3 (1.5, 2.9)	2.3 (1.5, 2.9)	2.2 (1.5, 2.9)	2.2 (1.5, 2.8)	2.2 (1.7, 2.8)	2.3 (1.7, 2.8)	2.3 (1.7, 2.8)
2	2.6 (1.9, 3.2)	2.5 (1.8, 3.3)	2.6 (1.9, 3.2)	2.6 (1.9, 3.2)	2.6 (2.1, 3.2)	2.6 (2.1, 3.2)	2.6 (2.1, 3.1)
3	2.6 (1.9, 3.3)	2.6 (1.8, 3.3)	2.6 (2.0, 3.3)	2.6 (2.0, 3.2)	2.6 (2.1, 3.2)	2.6 (2.1, 3.1)	2.6 (2.2, 3.1)
4	2.6 (1.8, 3.3)	2.6 (1.8, 3.3)	2.6 (1.8, 3.3)	2.6 (2.0, 3.2)	2.6 (2.0, 3.2)	2.6 (2.1, 3.1)	2.6 (2.1, 3.0)
5	2.6 (1.9, 3.2)	2.6 (1.9, 3.2)	2.6 (2.0, 3.3)	2.6 (1.9, 3.2)	2.6 (2.0, 3.2)	2.6 (2.1, 3.2)	2.6 (2.1, 3.1)
6	2.6 (1.9, 3.3)	2.6 (1.9, 3.3)	2.6 (1.9, 3.1)	2.6 (2.0, 3.2)	2.6 (2.0, 3.2)	2.6 (2.1, 3.2)	2.6 (2.1, 3.1)
7	2.6 (2.0, 3.2)	2.6 (1.8, 3.3)	2.6 (1.8, 3.2)	2.6 (2.0, 3.2)	2.6 (2.1, 3.3)	2.6 (2.1, 3.1)	2.6 (2.1, 3.1)
8	2.6 (1.9, 3.3)	2.6 (1.8, 3.3)	2.6 (1.9, 3.3)	2.6 (2.0, 3.2)	2.6 (2.0, 3.2)	2.6 (2.1, 3.1)	2.6 (2.2, 3.2)
9	2.6 (1.9, 3.4)	2.6 (1.9, 3.3)	2.6 (2.0, 3.3)	2.6 (1.9, 3.2)	2.6 (2.0, 3.1)	2.6 (2.1, 3.2)	2.6 (2.0, 3.1)
10	2.6 (1.8, 3.2)	2.6 (1.9, 3.3)	2.6 (1.9, 3.2)	2.6 (2.0, 3.3)	2.6 (2.0, 3.1)	2.6 (1.9, 3.1)	2.6 (2.1, 3.1)
Simulated serial intervals (Scenario-II: generation time approximated by serial intervals with mean 5.1 days)							
Isolation delay (d)	$R_e=3.0$	$R_e=2.5$	$R_e=2.0$	$R_e=1.5$	$R_e=1.0$	$R_e=0.5$	$R_e=0.3$
0	1.5 (0.8, 2.2)	1.5 (0.8, 2.2)	1.5 (0.7, 2.1)	1.5 (0.9, 2.1)	1.5 (1.0, 2.0)	1.5 (0.9, 1.9)	1.5 (1.0, 2.0)
1	2.3 (1.5, 3.0)	2.3 (1.7, 3.0)	2.3 (1.7, 3.0)	2.3 (1.6, 2.9)	2.3 (1.8, 2.8)	2.4 (1.9, 2.9)	2.3 (1.9, 2.7)
2	3.0 (2.4, 3.7)	3.0 (2.4, 3.5)	3.0 (2.3, 3.8)	3.0 (2.4, 3.6)	3.0 (2.5, 3.6)	3.1 (2.5, 3.6)	3.0 (2.5, 3.6)
3	3.5 (2.8, 4.3)	3.6 (2.8, 4.1)	3.5 (2.8, 4.1)	3.5 (2.9, 4.2)	3.6 (3.0, 4.1)	3.6 (3.0, 4.3)	3.5 (3.1, 4.0)
4	3.9 (3.2, 4.6)	4.0 (3.3, 4.6)	4.0 (3.2, 4.5)	4.0 (3.4, 4.6)	4.0 (3.4, 4.5)	4.0 (3.5, 4.5)	4.0 (3.5, 4.5)
5	4.3 (3.5, 5.0)	4.3 (3.5, 5.0)	4.3 (3.6, 4.8)	4.3 (3.7, 4.9)	4.4 (3.9, 4.9)	4.3 (3.7, 4.9)	4.3 (3.8, 4.9)
6	4.6 (3.8, 5.3)	4.5 (3.9, 5.2)	4.6 (3.8, 5.2)	4.5 (3.8, 5.2)	4.5 (3.9, 5.1)	4.5 (4.0, 5.0)	4.6 (4.0, 5.1)
7	4.7 (3.9, 5.5)	4.7 (4.0, 5.3)	4.7 (4.1, 5.3)	4.7 (4.2, 5.3)	4.7 (4.1, 5.2)	4.7 (4.2, 5.2)	4.7 (4.1, 5.2)
8	4.9 (4.1, 5.5)	4.9 (4.2, 5.5)	4.9 (4.1, 5.6)	4.8 (4.1, 5.5)	4.8 (4.2, 5.3)	4.9 (4.3, 5.4)	4.9 (4.3, 5.4)
9	4.9 (4.1, 5.6)	4.9 (4.2, 5.6)	4.9 (4.3, 5.6)	5.0 (4.2, 5.6)	4.9 (4.3, 5.6)	5.0 (4.4, 5.6)	4.9 (4.4, 5.5)
10	5.1 (4.2, 5.8)	5.0 (4.2, 5.8)	5.0 (4.3, 5.6)	5.0 (4.3, 5.6)	5.0 (4.4, 5.7)	5.0 (4.4, 5.6)	5.0 (4.5, 5.5)
Simulated serial intervals (Scenario-III: generation time approximated by serial intervals with mean 7.8 days)							
Isolation delay (d)	$R_e=3.0$	$R_e=2.5$	$R_e=2.0$	$R_e=1.5$	$R_e=1.0$	$R_e=0.5$	$R_e=0.3$
0	1.2 (0.3, 2.0)	1.3 (0.5, 2.1)	1.3 (0.5, 2.0)	1.3 (0.7, 2.1)	1.3 (0.7, 1.9)	1.3 (0.8, 1.9)	1.3 (0.6, 2.0)
1	2.4 (1.6, 3.1)	2.4 (1.7, 3.0)	2.4 (1.8, 3.1)	2.4 (1.9, 3.0)	2.5 (1.9, 3.1)	2.4 (1.9, 2.9)	2.4 (1.9, 3.1)
2	3.6 (2.8, 4.2)	3.5 (2.8, 4.3)	3.5 (2.8, 4.2)	3.5 (2.9, 4.1)	3.5 (2.8, 4.2)	3.6 (2.9, 4.1)	3.5 (2.9, 4.1)
3	4.6 (3.8, 5.4)	4.6 (3.9, 5.3)	4.6 (3.9, 5.2)	4.6 (4.0, 5.2)	4.6 (4.1, 5.2)	4.6 (4.1, 5.2)	4.6 (4.1, 5.1)
4	5.6 (4.9, 6.3)	5.6 (4.9, 6.4)	5.6 (5.0, 6.3)	5.6 (4.9, 6.2)	5.6 (5.0, 6.1)	5.7 (5.1, 6.1)	5.6 (5.1, 6.1)
5	6.5 (5.8, 7.3)	6.6 (5.8, 7.2)	6.6 (5.9, 7.2)	6.6 (5.9, 7.2)	6.5 (6.0, 7.0)	6.6 (5.9, 7.1)	6.6 (6.1, 7.1)
6	7.3 (6.6, 8.1)	7.3 (6.6, 7.9)	7.3 (6.6, 7.9)	7.3 (6.8, 7.9)	7.3 (6.8, 7.9)	7.3 (6.8, 7.9)	7.3 (6.8, 7.8)
7	7.7 (6.8, 8.4)	7.8 (7.0, 8.5)	7.7 (7.1, 8.4)	7.7 (7.1, 8.2)	7.7 (7.1, 8.4)	7.7 (7.1, 8.2)	7.7 (7.1, 8.2)
8	7.8 (7.0, 8.5)	7.8 (7.0, 8.6)	7.8 (7.1, 8.5)	7.8 (7.2, 8.4)	7.8 (7.2, 8.3)	7.8 (7.3, 8.3)	7.8 (7.3, 8.3)
9	7.8 (6.9, 8.5)	7.8 (7.1, 8.5)	7.8 (7.1, 8.4)	7.8 (7.2, 8.4)	7.8 (7.2, 8.3)	7.8 (7.2, 8.4)	7.8 (7.3, 8.3)
10	7.8 (7.1, 8.5)	7.8 (7.1, 8.4)	7.8 (7.0, 8.5)	7.8 (7.2, 8.3)	7.8 (7.1, 8.4)	7.8 (7.3, 8.3)	7.8 (7.3, 8.4)
Simulated serial intervals (Scenario-IV: generation time approximated by serial intervals with mean 8.4 days)							

Isolation delay (d)	$R_e=3.0$	$R_e=2.5$	$R_e=2.0$	$R_e=1.5$	$R_e=1.0$	$R_e=0.5$	$R_e=0.3$
0	1.2 (0.4, 2.1)	1.2 (0.4, 2.0)	1.3 (0.4, 2.0)	1.2 (0.5, 1.7)	1.3 (0.6, 1.9)	1.2 (0.6, 1.9)	1.2 (0.5, 2.0)
1	2.4 (1.5, 3.1)	2.3 (1.7, 3.0)	2.3 (1.6, 3.0)	2.4 (1.6, 3.0)	2.4 (1.9, 3.0)	2.3 (1.7, 2.9)	2.4 (1.7, 3.1)
2	3.4 (2.7, 4.3)	3.5 (2.7, 4.2)	3.5 (2.8, 4.2)	3.5 (2.8, 4.2)	3.5 (2.9, 4.0)	3.5 (2.9, 3.9)	3.4 (2.9, 4.0)
3	4.6 (3.8, 5.3)	4.5 (3.8, 5.2)	4.6 (4.0, 5.2)	4.6 (4.0, 5.1)	4.6 (4.1, 5.1)	4.5 (4.1, 5.0)	4.5 (4.0, 5.0)
4	5.6 (4.8, 6.3)	5.7 (5.0, 6.3)	5.7 (5.0, 6.4)	5.6 (5.0, 6.2)	5.6 (5.0, 6.1)	5.6 (5.0, 6.2)	5.6 (5.1, 6.1)
5	6.6 (5.9, 7.5)	6.6 (5.8, 7.4)	6.6 (5.9, 7.2)	6.6 (6.1, 7.3)	6.6 (6.1, 7.2)	6.6 (6.0, 7.1)	6.6 (6.1, 7.1)
6	7.5 (6.8, 8.2)	7.5 (6.8, 8.1)	7.5 (6.8, 8.1)	7.5 (7.0, 8.1)	7.5 (6.9, 8.1)	7.5 (7.0, 8.0)	7.5 (7.1, 8.1)
7	8.2 (7.5, 8.9)	8.1 (7.4, 8.7)	8.2 (7.4, 8.9)	8.1 (7.5, 8.7)	8.1 (7.5, 8.7)	8.2 (7.6, 8.6)	8.1 (7.6, 8.7)
8	8.4 (7.5, 9.2)	8.4 (7.7, 9.0)	8.4 (7.7, 9.1)	8.4 (7.9, 8.9)	8.4 (7.8, 9.0)	8.4 (7.8, 9.0)	8.4 (7.8, 8.9)
9	8.4 (7.6, 9.1)	8.4 (7.8, 9.1)	8.4 (7.6, 9.0)	8.4 (7.8, 9.0)	8.4 (7.9, 9.0)	8.4 (7.9, 8.9)	8.4 (7.8, 9.0)
10	8.4 (7.6, 9.1)	8.4 (7.6, 9.1)	8.4 (7.8, 9.0)	8.4 (7.7, 8.9)	8.4 (7.8, 9.1)	8.4 (7.8, 8.9)	8.4 (7.8, 8.9)

**Table S5:** Proportions of variance in empirical serial intervals explained by the potential factors from the multi-variable regression models.

Models (Factors)	Household transmissions			Non-household transmissions			All transmissions		
	$R^2$	$\% \Delta R^2$	$df$	$R^2$	$\% \Delta R^2$	$df$	$R^2$	$\% \Delta R^2$	$df$
<b>Isolation delay</b> <sup>†</sup>	0.3859		23 <sup>§</sup>	0.4685		23 <sup>§</sup>	0.5151	-	34 <sup>§</sup>
+ <b>Isolation of suspected</b> *	0.4255	3.96	22	0.7663	29.78	22 <sup>§</sup>	0.6716	15.64	33
+ <b>Isolation of confirmed</b> *	0.4269	4.10	22	0.7643	29.59	22 <sup>§</sup>	0.6711	15.60	33
+ <b>Inter-city travel ban</b> *	0.3987	1.28	22	0.7317	26.32	22 <sup>§</sup>	0.6473	13.22	33 <sup>§</sup>
+ <b>Intra-city travel ban</b> *	0.4045	1.86	22	0.7278	25.93	22 <sup>§</sup>	0.6557	14.06	33 <sup>§</sup>
+ <b>Closure of public services</b> *	0.4267	4.08	22	0.7734	30.50	22 <sup>§</sup>	0.6823	16.72	33
+ <b>Closure of entertainment venues</b> *	0.4257	3.98	22	0.7685	30.00	22 <sup>§</sup>	0.6765	16.14	33
+ <b>Social mobilization</b> *	0.4135	2.76	22	0.7547	28.62	22 <sup>§</sup>	0.6724	15.73	33

<sup>†</sup> Basic Model: Predicting empirical serial intervals by accounting for isolation delay only.

\* Models improved by combining the basic model with each factor.

<sup>§</sup> Statistically significant (both the coefficients for isolation delay and additional factors)

$\% \Delta R^2$  measures the change in the explained variance from the model in comparison to the basic model.

i.e.  $\% \Delta R^2 = (R^2_{models} - R^2_{basic\ model}) \times 100$

## References and Notes

1. World Health Organization (WHO), “Coronavirus disease 2019 (COVID-19): Situation report – 162” (WHO, 2020); [www.who.int/docs/default-source/coronaviruse/situation-reports/20200629-covid-19-sitrep-161.pdf?sfvrsn=74fde64e\\_2](http://www.who.int/docs/default-source/coronaviruse/situation-reports/20200629-covid-19-sitrep-161.pdf?sfvrsn=74fde64e_2).
2. M. U. G. Kraemer, C.-H. Yang, B. Gutierrez, C.-H. Wu, B. Klein, D. M. Pigott, Open COVID-19 Data Working Group, L. du Plessis, N. R. Faria, R. Li, W. P. Hanage, J. S. Brownstein, M. Layan, A. Vespignani, H. Tian, C. Dye, O. G. Pybus, S. V. Scarpino, The effect of human mobility and control measures on the COVID-19 epidemic in China. *Science* **368**, 493–497 (2020). [doi:10.1126/science.abb4218](https://doi.org/10.1126/science.abb4218) [Medline](#)
3. C. Wenham, J. Smith, R. Morgan, Gender and COVID-19 Working Group, COVID-19: The gendered impacts of the outbreak. *Lancet* **395**, 846–848 (2020). [doi:10.1016/S0140-6736\(20\)30526-2](https://doi.org/10.1016/S0140-6736(20)30526-2) [Medline](#)
4. J. M. Jin, P. Bai, W. He, F. Wu, X.-F. Liu, D.-M. Han, S. Liu, J.-K. Yang, Gender Differences in Patients With COVID-19: Focus on Severity and Mortality. *Front. Public Health* **8**, 152 (2020). [doi:10.3389/fpubh.2020.00152](https://doi.org/10.3389/fpubh.2020.00152) [Medline](#)
5. J. Hellewell, S. Abbott, A. Gimma, N. I. Bosse, C. I. Jarvis, T. W. Russell, J. D. Munday, A. J. Kucharski, W. J. Edmunds, Centre for the Mathematical Modelling of Infectious Diseases COVID-19 Working Group, S. Funk, R. M. Eggo, Feasibility of controlling COVID-19 outbreaks by isolation of cases and contacts. *Lancet Glob. Health* **8**, e488–e496 (2020). [doi:10.1016/S2214-109X\(20\)30074-7](https://doi.org/10.1016/S2214-109X(20)30074-7) [Medline](#)
6. L. Ferretti, C. Wymant, M. Kendall, L. Zhao, A. Nurtay, L. Abeler-Dörner, M. Parker, D. Bonsall, C. Fraser, Quantifying SARS-CoV-2 transmission suggests epidemic control with digital contact tracing. *Science* **368**, eabb6936 (2020). [doi:10.1126/science.abb6936](https://doi.org/10.1126/science.abb6936) [Medline](#)
7. R. Armitage, L. B. Nellums, COVID-19 and the consequences of isolating the elderly. *Lancet Public Health* **5**, e256 (2020). [doi:10.1016/S2468-2667\(20\)30061-X](https://doi.org/10.1016/S2468-2667(20)30061-X) [Medline](#)
8. R. M. Anderson, H. Heesterbeek, D. Klinkenberg, T. D. Hollingsworth, How will country-based mitigation measures influence the course of the COVID-19 epidemic? *Lancet* **395**, 931–934 (2020). [doi:10.1016/S0140-6736\(20\)30567-5](https://doi.org/10.1016/S0140-6736(20)30567-5) [Medline](#)
9. J. R. Koo, A. R. Cook, M. Park, Y. Sun, H. Sun, J. T. Lim, C. Tam, B. L. Dickens, Interventions to mitigate early spread of SARS-CoV-2 in Singapore: A modelling study. *Lancet Infect. Dis.* **20**, 678–688 (2020). [doi:10.1016/S1473-3099\(20\)30162-6](https://doi.org/10.1016/S1473-3099(20)30162-6) [Medline](#)
10. K. Prem, Y. Liu, T. W. Russell, A. J. Kucharski, R. M. Eggo, N. Davies, Centre for the Mathematical Modelling of Infectious Diseases COVID-19 Working Group, M. Jit, P. Klepac, The effect of control strategies to reduce social mixing on outcomes of the COVID-19 epidemic in Wuhan, China: A modelling study. *Lancet Public Health* **5**, e261–e270 (2020). [doi:10.1016/S2468-2667\(20\)30073-6](https://doi.org/10.1016/S2468-2667(20)30073-6) [Medline](#)
11. M. A. Vink, M. C. Bootsma, J. Wallinga, Serial intervals of respiratory infectious diseases: A systematic review and analysis. *Am. J. Epidemiol.* **180**, 865–875 (2014). [doi:10.1093/aje/kwu209](https://doi.org/10.1093/aje/kwu209) [Medline](#)

12. J. T. Wu, K. Leung, G. M. Leung, Nowcasting and forecasting the potential domestic and international spread of the 2019-nCoV outbreak originating in Wuhan, China: A modelling study. *Lancet* **395**, 689–697 (2020). [doi:10.1016/S0140-6736\(20\)30260-9](https://doi.org/10.1016/S0140-6736(20)30260-9) [Medline](#)
13. M. Chinazzi, J. T. Davis, M. Ajelli, C. Gioannini, M. Litvinova, S. Merler, A. Pastore Y Piontti, K. Mu, L. Rossi, K. Sun, C. Viboud, X. Xiong, H. Yu, M. E. Halloran, I. M. Longini Jr., A. Vespignani, The effect of travel restrictions on the spread of the 2019 novel coronavirus (COVID-19) outbreak. *Science* **368**, 395–400 (2020). [doi:10.1126/science.aba9757](https://doi.org/10.1126/science.aba9757) [Medline](#)
14. H. Nishiura, N. M. Linton, A. R. Akhmetzhanov, Serial interval of novel coronavirus (COVID-19) infections. *Int. J. Infect. Dis.* **93**, 284–286 (2020). [doi:10.1016/j.ijid.2020.02.060](https://doi.org/10.1016/j.ijid.2020.02.060) [Medline](#)
15. H. Y. Cheng, S.-W. Jian, D.-P. Liu, T.-C. Ng, W.-T. Huang, H.-H. Lin, Taiwan COVID-19 Outbreak Investigation Team, Contact Tracing Assessment of COVID-19 Transmission Dynamics in Taiwan and Risk at Different Exposure Periods Before and After Symptom Onset. *JAMA Intern. Med.* 10.1001/jamainternmed.2020.2020 (2020). [doi:10.1001/jamainternmed.2020.2020](https://doi.org/10.1001/jamainternmed.2020.2020) [Medline](#)
16. Z. Du, X. Xu, Y. Wu, L. Wang, B. J. Cowling, L. A. Meyers, Serial Interval of COVID-19 among Publicly Reported Confirmed Cases. *Emerg. Infect. Dis.* **26**, 1341–1343 (2020). [doi:10.3201/eid2606.200357](https://doi.org/10.3201/eid2606.200357) [Medline](#)
17. Q. Li, X. Guan, P. Wu, X. Wang, L. Zhou, Y. Tong, R. Ren, K. S. M. Leung, E. H. Y. Lau, J. Y. Wong, X. Xing, N. Xiang, Y. Wu, C. Li, Q. Chen, D. Li, T. Liu, J. Zhao, M. Liu, W. Tu, C. Chen, L. Jin, R. Yang, Q. Wang, S. Zhou, R. Wang, H. Liu, Y. Luo, Y. Liu, G. Shao, H. Li, Z. Tao, Y. Yang, Z. Deng, B. Liu, Z. Ma, Y. Zhang, G. Shi, T. T. Y. Lam, J. T. Wu, G. F. Gao, B. J. Cowling, B. Yang, G. M. Leung, Z. Feng, Early Transmission Dynamics in Wuhan, China, of Novel Coronavirus-Infected Pneumonia. *N. Engl. J. Med.* **382**, 1199–1207 (2020). [doi:10.1056/NEJMoa2001316](https://doi.org/10.1056/NEJMoa2001316) [Medline](#)
18. J. M. Griffin, A. B. Collins, K. Hunt, D. McEvoy, M. Casey, A. W. Byrne, C. G. McAloon, A. Barber, E. A. Lane, S. J. More, A rapid review of available evidence on the serial interval and generation time of COVID-19. medRxiv 2020.05.08.20095075 [Preprint]. 11 May 2020. <https://doi.org/10.1101/2020.05.08.20095075>.
19. S. Ma, J. Zhang, M. Zeng, Q. Yun, W. Guo, Y. Zheng, S. Zhao, M. H. Wang, Z. Yang, Epidemiological parameters of coronavirus disease 2019: A pooled analysis of publicly reported individual data of 1155 cases from seven countries. medRxiv 2020.03.21.20040329 [Preprint]. 24 March 2020. <https://doi.org/10.1101/2020.03.21.20040329>.
20. X. He, E. H. Y. Lau, P. Wu, X. Deng, J. Wang, X. Hao, Y. C. Lau, J. Y. Wong, Y. Guan, X. Tan, X. Mo, Y. Chen, B. Liao, W. Chen, F. Hu, Q. Zhang, M. Zhong, Y. Wu, L. Zhao, F. Zhang, B. J. Cowling, F. Li, G. M. Leung, Temporal dynamics in viral shedding and transmissibility of COVID-19. *Nat. Med.* **26**, 672–675 (2020). [doi:10.1038/s41591-020-0869-5](https://doi.org/10.1038/s41591-020-0869-5) [Medline](#)
21. Q. Bi, Y. Wu, S. Mei, C. Ye, X. Zou, Z. Zhang, X. Liu, L. Wei, S. A. Truelove, T. Zhang, W. Gao, C. Cheng, X. Tang, X. Wu, Y. Wu, B. Sun, S. Huang, Y. Sun, J. Zhang, T. Ma, J.



- Lessler, T. Feng, Epidemiology and transmission of COVID-19 in 391 cases and 1286 of their close contacts in Shenzhen, China: A retrospective cohort study. *Lancet Infect. Dis.* **20**, 911–919 (2020). [doi:10.1016/S1473-3099\(20\)30287-5](https://doi.org/10.1016/S1473-3099(20)30287-5) [Medline](#)
22. J. Zhang, M. Litvinova, Y. Liang, Y. Wang, W. Wang, S. Zhao, Q. Wu, S. Merler, C. Viboud, A. Vespignani, M. Ajelli, H. Yu, Changes in contact patterns shape the dynamics of the COVID-19 outbreak in China. *Science* **368**, 1481–1486 (2020). [doi:10.1126/science.abb8001](https://doi.org/10.1126/science.abb8001) [Medline](#)
  23. Lin, PDGLin/COVID19\_EffSerialInterval\_NPI: Serial interval of SARS-CoV-2 was shortened over time by non-pharmaceutical interventions, version v1.0, Zenodo (2020); <http://doi.org/10.5281/zenodo.3940300>.
  24. H. Tian, Y. Liu, Y. Li, C.-H. Wu, B. Chen, M. U. G. Kraemer, B. Li, J. Cai, B. Xu, Q. Yang, B. Wang, P. Yang, Y. Cui, Y. Song, P. Zheng, Q. Wang, O. N. Bjornstad, R. Yang, B. T. Grenfell, O. G. Pybus, C. Dye, An investigation of transmission control measures during the first 50 days of the COVID-19 epidemic in China. *Science* **368**, 638–642 (2020). [doi:10.1126/science.abb6105](https://doi.org/10.1126/science.abb6105) [Medline](#)
  25. K. Leung, J. T. Wu, D. Liu, G. M. Leung, First-wave COVID-19 transmissibility and severity in China outside Hubei after control measures, and second-wave scenario planning: A modelling impact assessment. *Lancet* **395**, 1382–1393 (2020). [doi:10.1016/S0140-6736\(20\)30746-7](https://doi.org/10.1016/S0140-6736(20)30746-7) [Medline](#)
  26. A. Pan, L. Liu, C. Wang, H. Guo, X. Hao, Q. Wang, J. Huang, N. He, H. Yu, X. Lin, S. Wei, T. Wu, Association of Public Health Interventions With the Epidemiology of the COVID-19 Outbreak in Wuhan, China. *JAMA* **323**, 1915–1923 (2020). [doi:10.1001/jama.2020.6130](https://doi.org/10.1001/jama.2020.6130) [Medline](#)
  27. J. Zhang, M. Litvinova, W. Wang, Y. Wang, X. Deng, X. Chen, M. Li, W. Zheng, L. Yi, X. Chen, Q. Wu, Y. Liang, X. Wang, J. Yang, K. Sun, I. M. Longini Jr., M. E. Halloran, P. Wu, B. J. Cowling, S. Merler, C. Viboud, A. Vespignani, M. Ajelli, H. Yu, Evolving epidemiology and transmission dynamics of coronavirus disease 2019 outside Hubei province, China: A descriptive and modelling study. *Lancet Infect. Dis.* **20**, 793–802 (2020). [doi:10.1016/S1473-3099\(20\)30230-9](https://doi.org/10.1016/S1473-3099(20)30230-9) [Medline](#)
  28. A. Cori, N. M. Ferguson, C. Fraser, S. Cauchemez, A new framework and software to estimate time-varying reproduction numbers during epidemics. *Am. J. Epidemiol.* **178**, 1505–1512 (2013). [doi:10.1093/aje/kwt133](https://doi.org/10.1093/aje/kwt133) [Medline](#)
  29. L. Zou, F. Ruan, M. Huang, L. Liang, H. Huang, Z. Hong, J. Yu, M. Kang, Y. Song, J. Xia, Q. Guo, T. Song, J. He, H.-L. Yen, M. Peiris, J. Wu, SARS-CoV-2 Viral Load in Upper Respiratory Specimens of Infected Patients. *N. Engl. J. Med.* **382**, 1177–1179 (2020). [doi:10.1056/NEJMc2001737](https://doi.org/10.1056/NEJMc2001737) [Medline](#)
  30. Y. Pan, D. Zhang, P. Yang, L. L. M. Poon, Q. Wang, Viral load of SARS-CoV-2 in clinical samples. *Lancet Infect. Dis.* **20**, 411–412 (2020). [doi:10.1016/S1473-3099\(20\)30113-4](https://doi.org/10.1016/S1473-3099(20)30113-4) [Medline](#)
  31. X. K. Xu, X.-F. Liu, Y. Wu, S. T. Ali, Z. Du, P. Bosetti, E. H. Y. Lau, B. J. Cowling, L. Wang, Reconstruction of Transmission Pairs for novel Coronavirus Disease 2019 (COVID-19) in mainland China: Estimation of Super-spreading Events, Serial Interval,

- and Hazard of Infection. *Clin. Infect. Dis.* 10.1093/cid/ciaa790 (2020).  
[doi:10.1093/cid/ciaa790](https://doi.org/10.1093/cid/ciaa790) [Medline](#)
32. P. Trapman, F. Ball, J.-S. Dhersin, V. C. Tran, J. Wallinga, T. Britton, Inferring  $R_0$  in emerging epidemics-the effect of common population structure is small. *J. R. Soc. Interface* **13**, 20160288 (2016). [doi:10.1098/rsif.2016.0288](https://doi.org/10.1098/rsif.2016.0288) [Medline](#)
  33. S. W. Park, D. Champredon, J. Dushoff, Inferring generation-interval distributions from contact-tracing data. *J. R. Soc. Interface* **17**, 20190719 (2020).  
[doi:10.1098/rsif.2019.0719](https://doi.org/10.1098/rsif.2019.0719) [Medline](#)
  34. Q. H. Liu, M. Ajelli, A. Aleta, S. Merler, Y. Moreno, A. Vespignani, Measurability of the epidemic reproduction number in data-driven contact networks. *Proc. Natl. Acad. Sci. U.S.A.* **115**, 12680–12685 (2018). [doi:10.1073/pnas.1811115115](https://doi.org/10.1073/pnas.1811115115) [Medline](#)
  35. Y. Bai, L. Yao, T. Wei, F. Tian, D.-Y. Jin, L. Chen, M. Wang, Presumed Asymptomatic Carrier Transmission of COVID-19. *JAMA* **323**, 1406–1407 (2020).  
[doi:10.1001/jama.2020.2565](https://doi.org/10.1001/jama.2020.2565) [Medline](#)
  36. X. Pan, D. Chen, Y. Xia, X. Wu, T. Li, X. Ou, L. Zhou, J. Liu, Asymptomatic cases in a family cluster with SARS-CoV-2 infection. *Lancet Infect. Dis.* **20**, 410–411 (2020).  
[doi:10.1016/S1473-3099\(20\)30114-6](https://doi.org/10.1016/S1473-3099(20)30114-6) [Medline](#)
  37. M. M. Arons, K. M. Hatfield, S. C. Reddy, A. Kimball, A. James, J. R. Jacobs, J. Taylor, K. Spicer, A. C. Bardossy, L. P. Oakley, S. Tanwar, J. W. Dyal, J. Harney, Z. Chisty, J. M. Bell, M. Methner, P. Paul, C. M. Carlson, H. P. McLaughlin, N. Thornburg, S. Tong, A. Tamin, Y. Tao, A. Uehara, J. Harcourt, S. Clark, C. Brostrom-Smith, L. C. Page, M. Kay, J. Lewis, P. Montgomery, N. D. Stone, T. A. Clark, M. A. Honein, J. S. Duchin, J. A. Jernigan, Public Health–Seattle and King County and CDC COVID-19 Investigation Team, Presymptomatic SARS-CoV-2 Infections and Transmission in a Skilled Nursing Facility. *N. Engl. J. Med.* **382**, 2081–2090 (2020). [doi:10.1056/NEJMoa2008457](https://doi.org/10.1056/NEJMoa2008457) [Medline](#)
  38. T. Ganyani, C. Kremer, D. Chen, A. Torneri, C. Faes, J. Wallinga, N. Hens, Estimating the generation interval for coronavirus disease (COVID-19) based on symptom onset data, March 2020. *Euro Surveill.* **25**, 2000257 (2020). [doi:10.2807/1560-7917.ES.2020.25.17.2000257](https://doi.org/10.2807/1560-7917.ES.2020.25.17.2000257) [Medline](#)
  39. W. E. Wei, Z. Li, C. J. Chiew, S. E. Yong, M. P. Toh, V. J. Lee, Presymptomatic Transmission of SARS-CoV-2 - Singapore, January 23-March 16, 2020. *MMWR Morb. Mortal. Wkly. Rep.* **69**, 411–415 (2020). [doi:10.15585/mmwr.mm6914e1](https://doi.org/10.15585/mmwr.mm6914e1) [Medline](#)
  40. L. Tindale, M. Coombe, J. E. Stockdale, E. Garlock, W. Y. V. Lau, M. Saraswat, Y.-H. B. Lee, L. Zhang, D. Chen, J. Wallinga, C. Colijn, Transmission interval estimates suggest pre-symptomatic spread of COVID-19. medRxiv 2020.03.03.20029983 [Preprint]. 6 March 2020. <https://doi.org/10.1101/2020.03.03.20029983>.
  41. R. Wölfel, V. M. Corman, W. Guggemos, M. Seilmaier, S. Zange, M. A. Müller, D. Niemeyer, T. C. Jones, P. Vollmar, C. Rothe, M. Hoelscher, T. Bleicker, S. Brünink, J. Schneider, R. Ehmann, K. Zwirgmaier, C. Drosten, C. Wendtner, Virological assessment of hospitalized patients with COVID-2019. *Nature* **581**, 465–469 (2020).  
[doi:10.1038/s41586-020-2196-x](https://doi.org/10.1038/s41586-020-2196-x) [Medline](#)

42. A. T. Huang, B. Garcia-Carreras, M. D. T. Hitchings, B. Yang, L. Katzelnick, S. M. Rattigan, B. Borgert, C. Moreno, B. D. Solomon, I. Rodriguez-Barraquer, J. Lessler, H. Salje, D. S. Burke, A. Wesolowski, D. A. T. Cummings, A systematic review of antibody mediated immunity to coronaviruses: Antibody kinetics, correlates of protection, and association of antibody responses with severity of disease. medRxiv 2020.04.14.20065771 [Preprint]. 17 April 2020. <https://doi.org/10.1101/2020.04.14.20065771>.
43. B. Rockx, T. Kuiken, S. Herfst, T. Bestebroer, M. M. Lamers, B. B. Oude Munnink, D. de Meulder, G. van Amerongen, J. van den Brand, N. M. A. Okba, D. Schipper, P. van Run, L. Leijten, R. Sikkema, E. Verschoor, B. Verstrepen, W. Bogers, J. Langermans, C. Drosten, M. Fentener van Vlissingen, R. Fouchier, R. de Swart, M. Koopmans, B. L. Haagmans, Comparative pathogenesis of COVID-19, MERS, and SARS in a nonhuman primate model. *Science* **368**, 1012–1015 (2020). [doi:10.1126/science.abb7314](https://doi.org/10.1126/science.abb7314) [Medline](#)
44. M. Lipsitch, T. Cohen, B. Cooper, J. M. Robins, S. Ma, L. James, G. Gopalakrishna, S. K. Chew, C. C. Tan, M. H. Samore, D. Fisman, M. Murray, Transmission dynamics and control of severe acute respiratory syndrome. *Science* **300**, 1966–1970 (2003). [doi:10.1126/science.1086616](https://doi.org/10.1126/science.1086616) [Medline](#)
45. K. M. Gostic, L. McGough, E. Baskerville, S. Abbott, K. Joshi, C. Tedijanto, R. Kahn, R. Niehus, J. A. Hay, P. M. De Salazar, J. Hellewell, S. Meakin, J. Munday, N. Bosse, K. Sherratt, R. M. Thompson, L. F. White, J. Huisman, J. Scire, S. Bonhoeffer, T. Stadler, J. Wallinga, S. Funk, M. Lipsitch, S. Cobey, Practical considerations for measuring the effective reproductive number, Rt. medRxiv 2020.06.18.20134858 [Preprint]. 23 June 2020. <https://doi.org/10.1101/2020.06.18.20134858>.
46. J. Wallinga, P. Teunis, Different epidemic curves for severe acute respiratory syndrome reveal similar impacts of control measures. *Am. J. Epidemiol.* **160**, 509–516 (2004). [doi:10.1093/aje/kwh255](https://doi.org/10.1093/aje/kwh255) [Medline](#)
47. C. Fraser, Estimating individual and household reproduction numbers in an emerging epidemic. *PLOS ONE* **2**, e758 (2007). [doi:10.1371/journal.pone.0000758](https://doi.org/10.1371/journal.pone.0000758) [Medline](#)
48. Z. Li, Q. Chen, L. Feng, L. Rodewald, Y. Xia, H. Yu, R. Zhang, Z. An, W. Yin, W. Chen, Y. Qin, Z. Peng, T. Zhang, D. Ni, J. Cui, Q. Wang, X. Yang, M. Zhang, X. Ren, D. Wu, X. Sun, Y. Li, L. Zhou, X. Qi, T. Song, G. F. Gao, Z. Feng, China CDC COVID-19 Emergency Response Strategy Team, Active case finding with case management: The key to tackling the COVID-19 pandemic. *Lancet* **396**, 63–70 (2020). [doi:10.1016/S0140-6736\(20\)31278-2](https://doi.org/10.1016/S0140-6736(20)31278-2) [Medline](#)
49. P. Wu, X. Hao, E. H. Y. Lau, J. Y. Wong, K. S. M. Leung, J. T. Wu, B. J. Cowling, G. M. Leung, Real-time tentative assessment of the epidemiological characteristics of novel coronavirus infections in Wuhan, China, as at 22 January 2020. *Euro Surveill.* **25**, 2000044 (2020). [doi:10.2807/1560-7917.ES.2020.25.3.2000044](https://doi.org/10.2807/1560-7917.ES.2020.25.3.2000044) [Medline](#)